Variation in Radiosensitivities of Different Individuals to High Energy Neutrons and ^{60}Cobalt γ-rays

by

Philip Rudolph Beukes

Thesis presented in partial fulfilment of the requirements for the degree

Master of Science in Medical Sciences at

Stellenbosch University

Supervisor: Prof Jacobus Slabbert

Faculty of Medicine and Health Sciences

December 2012

Declaration

By submitting this thesis/dissertation electronically, I declare that the entirety of the work contained therein is my own, original work, that I am the sole author thereof (save to the extent explicitly otherwise stated), that reproduction and publication thereof by Stellenbosch University will not infringe any third party rights and that I have not previously in its entirety or in part submitted it for obtaining any qualification.

December 2012

Abstract

Background: The assignment of radiation weighting factors to high energy neutron sources is important as there is reason to believe that neutron relative biological effectiveness (RBE) may be related to the inherent radiosensitivity of different individuals. A study was undertaken to quantify the inherent radiosensitivities of lymphocytes obtained from different donors to ^{60}Co γ-rays and p(66)/Be neutrons. For this a novel semi-automated image analysis process has been employed. In addition the responses of lymphocytes with different inherent radiosensitivities have also been tested using Auger electrons emitted by ^{123}I.

Methods: The RBE of neutrons was determined from dose-response curves for lymphocytes from different donors. Isolated T-lymphocytes irradiated *in vitro* were cultured to induce micronuclei in binucleated cells and micronuclei (MN) formations numerated using a semi-automated Metafer microscope system. The accuracy in obtaining dose response curves with this method has been tested by evaluating dispersion parameters of MN formations in the response to the different treatment modalities. Differences in the inherent radiosensitivities of cells from different donors were ascertained using 95 % confidence ellipses. [^{123}I]Iododeoxyuridine was prepared in a formulation that allows incorporation of ^{123}I into the DNA of lymphocytes. Micronucleus formations to this treatment were evaluated in lymphocytes with established differences in inherent radiosensitivities.

Results: The image analysis system proved to be consistent in detecting micronuclei frequencies in binucleated lymphocytes. As a result, differences in the inherent radiosensitivities of different individuals were distinctive and could be stated at the 95% confidence level. The inter-individual radiosensitivity variations were considerably smaller for blood cells exposed to high energy neutrons compared to ^{60}Co γ-rays. Relative biological effectiveness (RBE_M) values between 2 and 13 were determined that are highly correlated with the inherent radioresistance of lymphocytes obtained from different individuals. As such radiation weighting factors for high energy neutrons cannot be based on cytogenetic damage determined in lymphocytes from a single donor. Dispersion parameters for micronuclei formations

proved to vary according to ionization density. The variation in RBE with neutron dose changed according to theoretical considerations and automated image analysis detection of MN is thus a suitable method to quantify radiation weighting factors.

A clear reduction in the variation in radiosensitivity is noted for lymphocytes exposed to Auger electrons compared to ^{60}Co γ-rays. The effectiveness of Auger electrons from [^{123}I]IUdR to induce biological damage is demonstrated as the number of disintegrations needed to yield micronuclei formations was found to be more than two orders of magnitude less than that of other compounds. An increase in the RBE of Auger electrons with radioresistance can be inferred from these findings and constitutes a basis for therapeutic gain in treating cells compared to using radioisotopes emitting low-LET radiation.

Opsomming

Agtergrond: Die bepaling van straling gewigsfaktore vir hoë energie neutron bronne is belangrik, aangesien daar rede is om te glo dat die relatiewe biologiese effektiwiteit (RBE) kan verband hou met die inherente stralings sensitiwiteit van verskillende individue. Hierdie studie is onderneem om die inherente radiosensitiwiteit van limfosiete verkry vanaf verskillende skenkers te kwantifiseer na blootstelling aan ^{60}Co γ-strale en p(66)/Be neutrone. Vir hierdie doel is daar van 'n semi-outomatiese beeldontleding metode gebruik gemaak. Daarbenewens is die reaksie van limfosiete met vooraf bepaalde inherente radiosensitiwiteite ook getoets aan die hand van Auger elektrone wat uitgestraal word deur ^{123}I.

Metodiek: Die RBE van neutrone was bepaal uit dosis mikrokerne frekwensie verwantskappe verkry vir limfosiete. Geïsoleerde T-limfosiete was *in vitro* bestraal en gekweek om mikrokerne te vorm in dubbelkernige selle. Die mikrokerne was gekwantifiseer deur die gebruik van 'n semi-outomatiese Metafer mikroskoop stelsel. Die akkuraatheid in die verkryging van dosis-effek krommes met hierdie metode is getoets deur die ontleding van verspreidings parameters van MN vorming in reaksie op behandeling met die verskillende stralings modaliteite. Verskille in die inherente stralingsensitiwiteite van die selle van verskillende skenkers was vasgestel deur die konstruksie van 95 % betroubaarheidsinterval ellipse. [^{123}I]Iododeoxyuridine was ook berei om ^{123}I in die DNA van limfosiete in te bou. Die mikrokerne vorming op die behandeling is beoordeel in limfosiete met gevestigde verskille in inherent radiosensitiwiteite.

Resultate: Die beeld analise stelsel bewys om konsekwent te wees in die opsporing van mikrokerne wat vorm in dubbelkernige limfosiete. Verskille in die inherente radiosensitiwiteite van verskillende skenkers kon vasgestel word op die 95 % betroubaarheidsvlak. Die skommeling in inter-individuele stralings sensitiwiteite was kleiner vir bloed selle blootgestel aan hoë-energie neutrone in vergelyking met ^{60}Co γ-strale. Relatiewe biologiese effektiwiteit (RBE_M) waardes tussen 2 en 13 is bepaal wat sterk verband hou met die inherente radioweerstandbiedendheid van limfosiete verkry vanaf verskillende persone. As sodanig kan straling gewigsfaktore vir hoë

energie neutrone nie gebaseer word op sitogenetiese skade in limfosiete van 'n enkele skenker nie. Verspreidings parameters vir mikrokern vorming het gewissel as ‘n funksie van ionisasiedigtheid van die straling. Die verandering in RBE met neutron dosis verloop volgens teoretiese oorwegings en die semi-outomatiese beeldontledings metode om mikrokerne op te spoor is dus geskik om stralings gewigsfaktore te kwantifiseer.

'n Duidelike afname in die verandering in die stralingsensitiwiteite is waargeneem vir limfosiete blootgestel aan Auger elektrone in vergelyking met ^{60}Co γ-strale. Die hoë doeltreffendheid van Auger elektrone afkomstig van [^{123}I]IUdR om biologiese skade te veroorsaak, word weerspieël deur die feit dat die getal disintegrasies wat nodig is om mikrokerne te vorm meer as twee ordes grootte minder is as dié van ander verbindings. 'n Toename in die RBE van Auger elektrone in selle wat radioweerstandbiedend is kan afgelei word uit hierdie bevindinge. Dit vorm 'n basis vir terapeutiese wins in die behandeling van selle in vergelyking met die gebruik van radio-isotope wat lae ionisasie digthede tot stand bring.

Acknowledgements

Most importantly I offer my genuine appreciation to my supervisor, Prof Slabbert. Without his support, knowledge and persistence this thesis would not have been written nor completed.

Also to the individuals who supported me throughout my studies:

Prof Verschoor, for stamping the visa in my passport for life.

To my colleagues:

Drs Veerle and Bram, for their expert opinion and assistance with the experimental work.

Julyan Symons for the assistance with the neutron irradiations.

Sr. Elmarie for her involvement with blood collections.

Also a big thank you to both De Vlaamse Interuniversitaire Raad (VLIR) and NRF iThemba LABS for providing the facilities and financial support vital to this research project.

A special thanks to my parents for their continued support.

Finally never enough thanks to my wife, for being my pillar of strength while facing her own demons.

Table of Contents

List of Figures

List of Tables

List of Abbreviations

ANOVA	- Analysis of Variance
AS	- Abasic Sites
BD	- Base Damage
BN	- Binucleated
BNC	- Binucleated Cell
CBMN	- Cytokinesis Block Micronucleus Assay
CCD	- Charge-Coupled Device
CHO	- Chinese Hamster Ovary
CV	- Coefficient of Variation
Cyt-B	- Cytochalasin-B
DAPI	- 4′, 6′-Diamidino-2-Phenylindole
DCA	- Dicentric Chromosome Assay
DMSO	- Dimethylsulphoxide
DNA	- Deoxyribonucleic Acid
DSB	- Double Strand Break
EDTA	- Ethylene Diamine Tetra Acetic Acid
FISH	- Fluorescence In Situ Hybridization
Fig	- Figure
g	- Relative centrifugal force
HPBL	- Human Peripheral Blood Lymphocytes
IAEA	- International Atomic Energy Agency

ICRP	- International Commission on Radiological Protection
ICRU	- International Commission on Radiation Units and Measurements
LET	- Linear Energy Transfer
MN	- Micronucleus (Micronuclei)
MNF	- Micronucleus Frequency (Micronuclei Frequencies)
NDI	- Nuclear Division Index
NHEJ	- Non-Homologous End-Joining
p(66)/Be	- 66 MeV Protons Incident On A Be Target
PBS	- Phosphate Buffered Saline
PCC	- Premature Chromosome Condensation
PHA	- Phytohaemagglutinin
RBE	- Relative Biological Effectiveness
SD	- Standard Deviation
SE	- Standard Error
SEM	- Standard Error of the Mean
SI	- International System of Units
SSB	- Single Strand Break
IUdR	- Iododeoxyuridine
γ-ray(s)	- Gamma Ray(s)

Chapter 1

Introduction

The biological effects of ionizing radiation are determined by both the radiation dose and the radiation quality (ionization density). To understand the radiation protection concerns associated with different types of ionizing radiation, knowledge of both the extent of exposure and consequent macroscopic absorbed dose, measured in gray, as well as the microscopic dose distribution of the radiation modality is required. The definitions of these variables are discussed below but in general to advance the knowledge of the biological effects of different radiation types one needs to know the dose absorbed, the radiation quality and effectiveness of a particular radiation type.

In this study the biological effect of high energy neutrons was compared to that of a reference radiation type ^{60}Co γ-rays for cells obtained from a cohort of donors, mostly radiation workers. Comparisons were made at different dose levels in blood cells from each donor to ascertain the relative biological effectiveness of the test radiation modality against that of a reference radiation (Lam, 1990). Such studies are essential to determine the radiation quality for high energy neutron sources applicable to practises in radiation protection.

In some nuclear medicine applications radionuclides are used to treat malignant disease. For this the use of short lived alpha particle emitters or other radiation modalities that deliver high ionization densities in cells, are particularly attractive. These modalities are used as the cellular response in relation to inherent radiosensitivity of the effected cells is thought to be more consistent compared to the use of radionuclides that emit radiation with a lower ionization density e.g. β-particles. The relative biological effectiveness of the high energy neutrons used in this study was tracked as a function of the inherent radiosensitivity of different individuals. This allows the identification of cell populations that are relatively sensitive or relatively resistant to radiation. Furthermore Auger electron emitting radionuclides, known to induce biological damage comparable to that of alpha

particles, are available at iThemba LABS; hence variations in the inherent radiosensitivity of cells obtained from different individuals were evaluated.

A short description of the physical and biological variables applicable to this study is summarised below.

Ionizing Radiation

Ionizing radiation refers to both uncharged particles (e.g., photons or neutrons) and charged particles (e.g., electrons or protons) that can deliver enough energy to atoms and molecules to cause ionizations. Ionization produced by particles is the process by which one or more electrons are removed from atoms or molecules in collisions with the particle (ICRU, 2011).

Interaction of Ionizing Radiation with Matter

The effects of ionizing radiation are not limited to ionization events. Other physical and chemical effects in matter such as: heat generation, excitation of atoms and molecules, destruction of chemical bonds, atomic displacements and nuclear reactions may occur. The effects of ionizing radiation on matter depend on the type and energy of radiation, the absorbing medium and the irradiation conditions (ICRU, 2011).

Radiation can be categorized in terms of how it induces ionizations:

- Directly ionizing radiation, consist of charged particles such as electrons, protons and alpha particles.
- Indirectly ionizing radiation consists of neutral particles such as neutrons and/or electromagnetic radiation such as photons (γ-rays and X-rays).

Ionising radiation interacts with matter by:

- Interaction with the electron cloud of the atom, or by
- Interaction with the nucleus of the atom.

Types of Ionizing Radiation Used In This Study

Ionizing Photons

Ionizing photons (X- and γ-rays) are categorised as indirectly ionising radiation. X- and γ-rays have zero rest mass and carry no electrical charge. Low energy photons with quantum energy less than the rest mass of two electrons ($E<2m_0c^2$), only interact with orbital electrons and give rise to fast moving secondary electrons (Grosswendt, 1999). The photons can be absorbed in photo-electric interactions or scattered and knock out atomic electrons in the process known as Compton scatter. If the energy of the incident photon exceeds 1.02 MeV the probability to create a pair of β^- β^+ particles in the pair production process dominates. Photons with very high energy ($E>>2m_0c^2$) may be absorbed by atomic nuclei and initiate nuclear reactions (Cember, 1969). The charged electrons emitted from the atoms, produce the excitation and ionisation events in the absorbing medium.

Neutrons

Neutrons are similar to ionizing photons in that they are indirectly ionizing. There is negligible interaction between neutrons and the electron cloud of atoms since neutrons do not have a net electrical charge (Henry, 1969). The principle interactions of these particles occur through direct collisions with atomic nuclei of the absorbing medium during elastic scattering events. In this process, ionization is produced by charged particles such as knock-on-protons recoil nuclei and nuclear reaction products. The production of secondary ionizing photons will result in the release of energetic electrons. In turn the secondary charged particles can deposit energy at a significant distance from the interaction sites (Pizzarello, 1982).

Auger Electrons

Auger electron emission is an atomic and not a nuclear process. In this process an electron is ejected from an orbital shell of the atom. Following electron capture (EC)

or internal conversion (IC) the atom is left with a vacant state in its electron configuration. An electron from a higher energy shell may drop into the vacant state and the energy difference will be emitted as a characteristic X-ray (Cember, 1969). The energy of the X-ray ($E_{X\text{-}ray}$) being the difference in energy (E) between the two electron shells L and K.

$$E_{X\text{-}ray} = E_L - E_K$$

Alternatively, the energy may be transferred to an electron of an outer shell, causing it to be ejected from the atom (Fig. 1.1). The emitted electron is known as an Auger electron and similarly to the X-ray has energy:

$$E_{Auger} = E_\Delta - E_B$$

where: E_Δ = the energy of inner-shell vacancy - energy of outer-shell vacancy
E_B = binding energy of emitted (Auger) electron

Auger electron emission is favoured for low-Z materials (e.g. ^{123}I) where electron binding energies are small. Auger electrons have low kinetic energies; hence travel only a very short range in the absorbing medium (Cember, 1969).

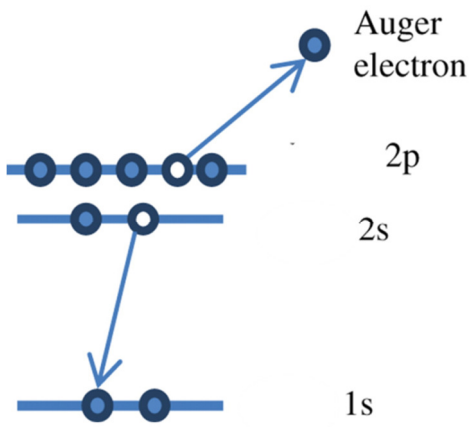

Figure 1.1: Schematic representation of the Auger electron emission process, where an orbital electron is ejected following an ionization event (Cerruti, 2011).

Dosimetric Quantities

Several dosimetric quantities have been defined to quantify energy deposition in a medium when ionizing radiation passes through it. Radiation fields are well described by physical quantities such as particle fluence or kerma in air. However these quantities do not describe the effects of exposure to ionizing radiation on biological systems (ICRP, 2007).

Absorbed dose (D) is used to quantify energy deposition by any type of radiation in any absorbing material. The International System of Units (SI) of absorbed dose is joule per kilogram ($J.kg^{-1}$) and is termed the gray (Gy).

Absorbed dose is defined as the quotient of the energy (dε) imparted by ionising radiation to matter with mass (dm) (Cember, 1969).

$$D = \frac{d\varepsilon}{dm}$$

Absorbed dose quantitatively describes the energy imparted per unit mass absorbing medium. This value is linked to the level of biological damage to cells or tissue but only within a specific radiation type. To connect the quantity, absorbed dose, to biological damage induced to biological systems by ionizing radiation, the radiation weighted dose (H_T) is used. It is calculated as:

$$H_T = \sum_R w_R D_{T,R}$$

where $D_{T,R}$ is the absorbed dose in a tissue T due to radiation of type R and w_R is the corresponding dimensionless radiation weighting factor for the specific radiation quality.

The unit of radiation weighted dose is $J.kg^{-1}$ and is named the sievert (Sv). Radiation weighting factors are recommended by the International Commission on Radiological

Protection (ICRP, 2007) and are derived from studies on the effect of the micro-deposition of radiation energy in tissue and on its carcinogenic potential.

Linear Energy Transfer

Ionizing radiation deposits energy in the form of ionizations along the track of the ionizing particle. The spatial distribution of these ionization events is related to the radiation type. The term linear energy transfer (LET) defines the average rate at which charged particles deposit energy in the absorbing medium per unit distance (keV/µm). LET is regarded as a realistic measure of radiation quality (Duncan and Nias, 1977).

LET of charged particles in an absorbing medium is defined as the quotient of *dE/dl* where *dE* is the energy deposited in the absorbing medium by a charged particle with defined energy over a distance *dl* (Pizzarello, 1982).

$$LET = \frac{dE}{dl}$$

For high energy photons, fast electrons are ejected when these interact with the absorbing medium. The primary ionization events along the track of the ionizing particle are well separated. This type of sparsely ionizing radiation is termed low-LET radiation. The LET of a ^{60}Cobalt teletherapy source (1.3325 and 1.1732 MeV) is in the range of 0.24 keV/µm (Vral *et al*., 1994).

Neutrons cause the emission of recoil protons, alpha particles and heavy nuclear fragments during scatter events. These charged particles interact more readily with the absorbing medium and cause densely spaced ionizing events along its tracks. The p(66)/Be neutron beam used in this study has an average ionization density of 20 keV/µm and hence is regarded as high-LET radiation (Slabbert *et al*., 1989).

Auger electrons emitted by ^{123}I travel very short distances, just a few nanometres, in the absorbing medium due to their low kinetic energies of a few hundred electron

volt. All the energy of these particles is liberated in small volumes over short track lengths. Ionization densities are therefore very high; up to 40 keV/µm which is comparable to high-LET alpha particles (Goddu *et al*., 1994).

Relative Biological Effectiveness

The degree of damage caused by ionizing radiation depends on the absorbed dose and on the radiation quality. Variances in the biological effects of different radiation qualities can be described in terms of the relative biological effectiveness (RBE). RBE defines the magnitude of biological response for a certain radiation quality compared to a distinct reference radiation. It is expressed in terms of the ratio (Luu and DuChateau, 2009):

$$RBE = \frac{\text{Dose(reference radiation) to attain a given level of biological damage for an endpoint}}{\text{Dose(test radiation) to achieve the same level of biological damage for the same endpoint}}$$

^{60}Co γ-rays is often used as the reference radiation.

Therefore, for the same dose neutrons will produce more biological damage compared to ^{60}Co γ-rays. The essential difference between these radiation modalities is in the micro deposition of energy. Furthermore, RBE varies as a function of the dose applied. An increase in RBE is noted for a decrease in dose. By evaluating dose response curves (Fig. 1.2), it is evident that the shoulder of the neutron curve is much less pronounced compared to the reference radiation curve. As such changes in the RBE of a test radiation are prominent at low doses (Hall and Giaccia, 2005).

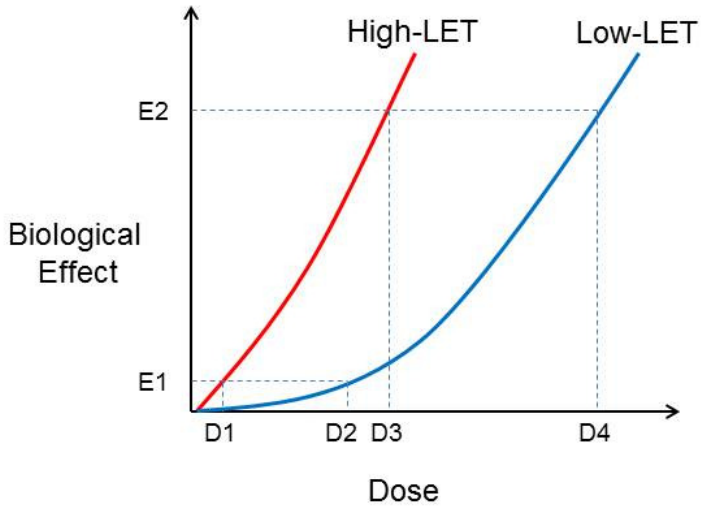

Figure 1.2: Dose response curves based on the linear quadratic model demonstrate differences in RBE as a function of dose (Hall and Giaccia, 2005).

Evaluation of the shape of dose/biological effect curves shows that the RBE for a specific radiation quality is dose dependant. The RBE increases with a decrease in dose, to reach a maximum RBE denoted RBE_M. This is calculated from the ratio of the initial slope of the dose response curves for both radiation modalities.

RBE is further influenced by the type of tissue or cells in which it is evaluated. Also this variable is determined by dose rate, oxygen status, the phase of the cell cycle and inherent radiosensitivity of cells. These factors influence the level of biological damage more in the reference radiation compared to that following exposure to the test radiation. As a result these factors influence the relative biological effectiveness of the test radiation.

RBE LET Relationship

With an increase in ionization density a specific dose of radiation is absorbed in cells using fewer tracks. In any track the number of ionizing events per unit distance increases with LET. Thus the probability of direct interaction between the particle track and target molecules in cells increases with ionization density.

The RBE of radiation can be correlated with the estimates of LET values. Below 10 keV/µm the RBE value is constant (Barendsen, 1968). However, when the LET exceeds 10 keV/µm it is no longer possible to assign a single value for RBE. Beyond this LET, the shapes of cell survival curves changes markedly with the result that RBE values increase systematically up to 100 keV/µm.

The average separation in ionizing events at a LET of 100 keV/µm is about equal to the width of deoxyribonucleic acid (DNA) double strand molecule (Fig. 1.3). Further increase in LET results in a decrease in RBE, since ionizing events occur at smaller intervals than the separation distance between the DNA molecule strands. Thus the additional energy imparted is effectively wasted and does not contribute to DNA damage.

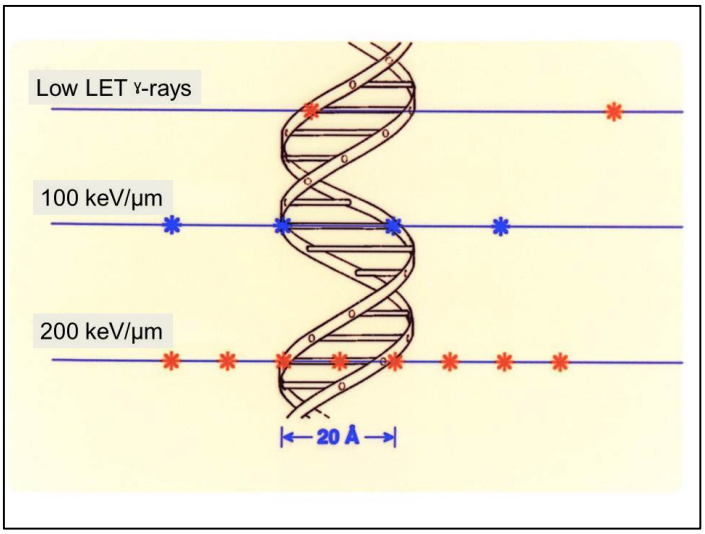

Figure 1.3: Average spatial distribution of ionizing events for different LET values in relation to the DNA double helix structure (Hall and Giaccia, 2005).

Cellular Radiosensitivity

In general cells in tissue that are more sensitive to radiation include those that are rapidly dividing (high mitotic activity), cells with a long dividing future (stem cells) and cells of an unspecialised type.

Ancel and Vitemberger later adapted the “law” of Bergonie and Tribondeau. They established that radiation damage was governed by two factors:

- the biological stress on the cell.
- pre and post irradiation conditions to which the cell is exposed.

A comprehensive system of classification of radiosensitivity was proposed by Rubin and Casarett in which cell populations were grouped into 4 categories based on the reproduction kinetics:

- Vegetative intermitotic cells were defined as rapidly dividing undifferentiated cells. These cells usually have a short life cycle. For example: erythroblasts and intestinal crypt cells and are very radiosensitive.
- Differentiating intermitotic cells are characterized as actively dividing cells with some level of differentiation. Examples include: myelocytes and midlevel cells in maturing cell lines, these cells are radiosensitive.
- Reverting postmitotic cells do not divide regularly and are generally long lived. Liver cells is an example of this cell type, these cell types exhibit a degree radioresistance.
- Fixed postmitotic cells do not divide. Cells belonging to this classification are regarded as being highly differentiated and highly specialized in both morphology and function. These cells are replaced by differentiating cells in the cell maturation lines and are regarded as the most radioresistant cell types. Nerve and muscle cells are prime examples (Hall and Giaccia, 2005).

Thus according to the above classifications undifferentiated rapidly dividing cells are most radiosensitive.

Cell Cycle Dependent Radiosensitivity

As cells progress through the cell cycle various physical and biochemical changes occur (Fig. 1.4). These changes influence the response of cells to ionizing radiation. In general following the law of Bergonie and Tribondeau which states that cells with high mitotic activity are most radiosensitive. Cells in the mitotic phase (M-phase) of

the cell cycle are most radiosensitive. Late stage gap 2 (G2-phase) cells are also very sensitive with gap 1 (G1-phase) being more radioresistant and synthesis (S-phase) cells the most radioresistant (Domon, 1980).

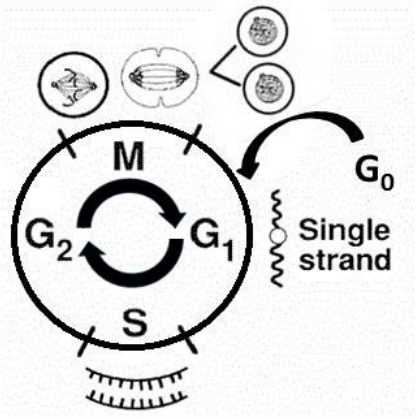

Figure 1.4: Schematic representation of the cell cycle. The G_0 resting phase for cells that do not actively proliferate is also shown since T-lymphocytes in their normal state are non-proliferating (Hall and Giaccia, 2005).

Non-proliferating cells may enter the rest phase G_0 from G_1 and remain inactive for long periods of time. Peripheral blood T-lymphocytes rarely replicate naturally and remain in G_0 indefinitely.

Lymphocyte Radiosensitivity

The hematopoietic system is very sensitive to radiation. Differential blood cell counts are routinely employed as a measure of radiation exposure. These measurements are based on the sensitivity of stem cells and the changes observed in the constituents of peripheral blood due to variations in transit time from stem cell to functioning cell (Hall and Giaccia, 2005).

It has been shown that lymphocytes do not meet the criteria of a radiation sensitive cell type. Lymphocytes are resting cells (G_0 phase) that do not actively proliferate nor do they have a long dividing future. Even so these cells are sensitive to radiation but the reasons for this are not fully explained (Hall and Giaccia, 2005).

T-lymphocytes have two distinct subpopulations with different inherent radiosensitivity. CD 8 cells are generally more sensitive than CD 4 cells (Kataoka and Sado, 1974, Knox *et al*., 1982).

Cytogenetic Expression of Ionizing Radiation Induced Damage

The primary target for ionizing radiation is the double helix deoxyribonucleic acid (DNA) molecule (Burdak-Rothkamm and Prise, 2009). This macro molecule contains the genetic code which is critical to the development and functioning of most living organisms. The DNA molecule consists of two strands held together by hydrogen bonds between the bases. Each strand is made up of four types of nucleotides. A nucleotide consists of a five-carbon sugar (deoxyribose), a phosphate group and a nitrogen containing base. The nitrogen containing bases are adenine, guanine, thymine or cytosine. Base pairing between two nucleotide strands is universally constant with adenine pairing with thymine and guanine with cytosine (Fig. 1.5). This attribute permits effective single strand break repair since the opposite strand is used as a template during the repair process. The base sequence within a nucleotide strand differs; the arrangement of bases defines the genetic code. The double helix DNA molecule is wound up on histones and bound together by proteins to form nucleosomes. This structure is folded and coiled repeatedly to become a chromosome.

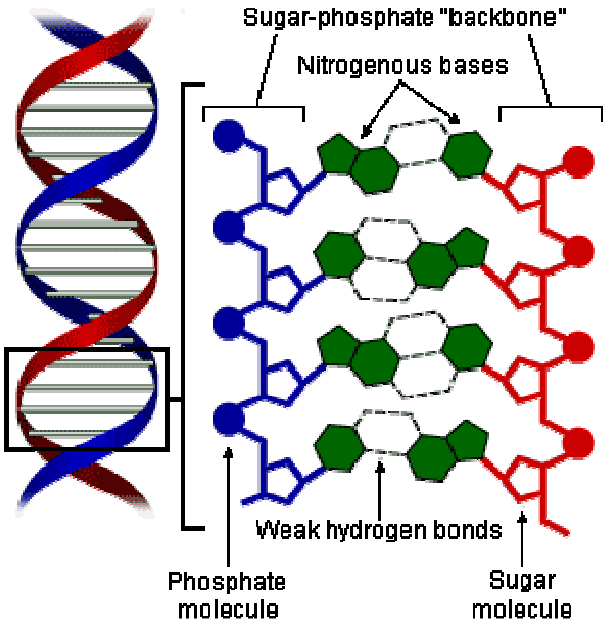

Figure 1.5: The double helix structure of a DNA molecule consists of two nucleotide strands held together by hydrogen bonds between the bases (Hall and Giaccia, 2005).

Ionizing radiation can either interact directly or indirectly with the DNA strand. When an ionization event occurs in close proximity to the DNA molecule direct ionization can denature the strand. Ionization events that occur within the medium surrounding the DNA produce free radicals such as hydrogen peroxide through radiolysis of water. Damage induced by ionizing radiation to the DNA include base damage (BD), single strand breaks (SSB), abasic sites (AS), DNA-protein cross-links (DPC), and double strand breaks (DSB) (Fig. 1.6).

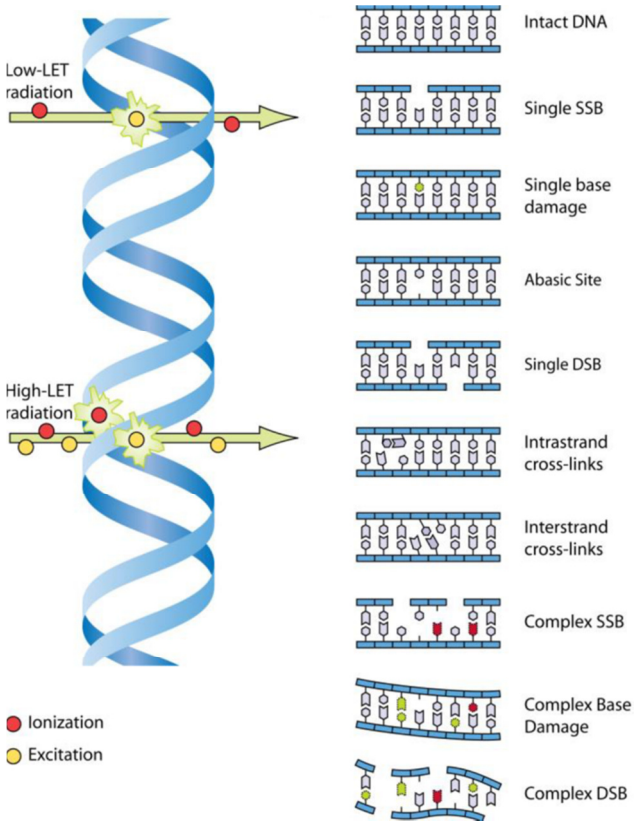

Figure 1.6: Examples of several radiation induced DNA lesions (IAEA, 2011).

More than one track of low-LET radiation is generally required to induce a double strand break. High-LET radiation damage is dominated by direct interactions with the DNA molecule producing double strand breaks within a single track. Densely ionizing radiation has a greater probability to induce irreparable or lethal damage.

Several techniques to quantify chromosomal damage and chromatid breaks have been established. These range from isolating DNA and passing it through a porous substrate or gel by applying an external potential difference to advanced techniques of visually observing and enumerating chromosomal aberrations of interphase cells (IAEA, 2011).

Cytogenetic chromosome aberration assays for peripheral blood lymphocytes include premature chromosome condensation (PCC), metaphase spread dicentric and ring chromosome analysis (DCA), metaphase spread fluorescence in situ

hybridisation (FISH) translocation detection and cytokinesis blocked micronuclei (CBMN) counting (Fig. 1.7).

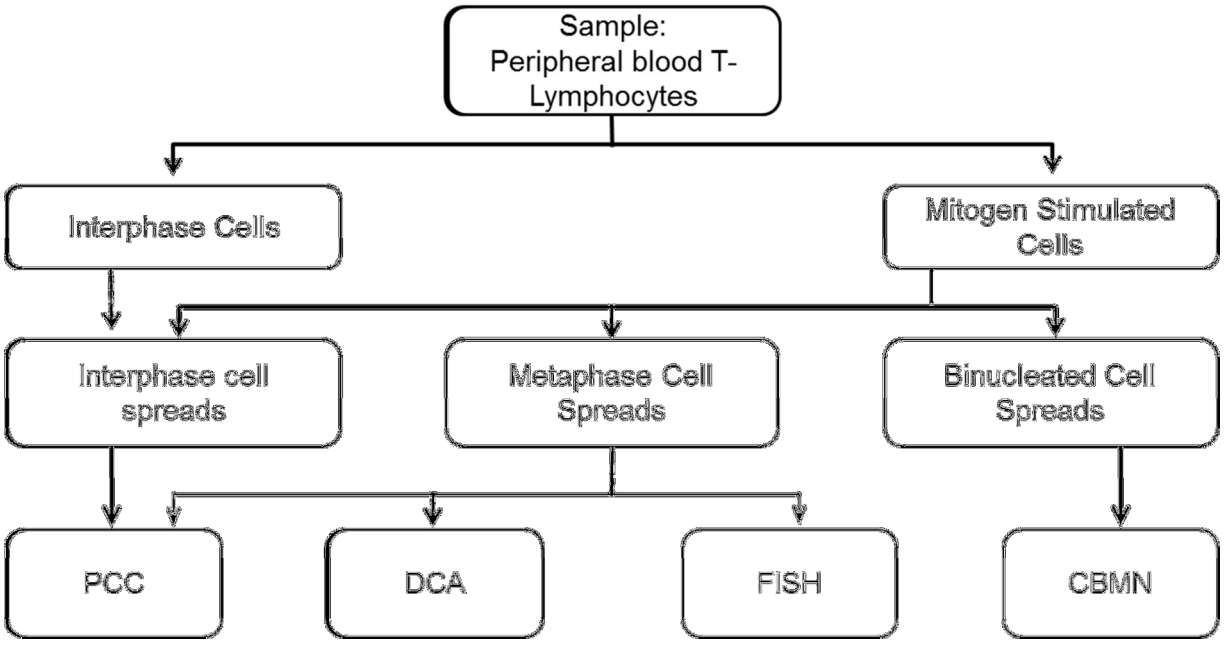

Figure 1.7: Different cytogenetic assays on peripheral T-lymphocytes for use in biological dosimetry (IAEA, 2011).

PCC involves the use of a fusing technique of interphase cells with mitotic cells. The fusion causes interphase cells to prematurely condense chromosomes. This happens within hours of exposures and chromosomal aberrations can thus be analysed immediately following irradiation without the need for mitogen stimulation or cell culturing.

Enumeration of dicentrics in metaphase spreads has been used with great success to assess radiation damage in lymphocytes since the 1960's (Vral *et al.*, 2011). The incidence of these aberrations follows a linear quadratic response with respect to the dose. Unstable aberrations like dicentrics or centric rings are lethal to the cell hence do not passed on to daughter cells. By contrast translocations are stable aberrations that are not lethal to the cell and can be passed on to daughter cells. Examination of translocations thus provides a long term history of exposure to ionizing radiation.

Although the abovementioned techniques are very accurate and well described, the complexity and time consuming nature of the assays has stimulated the development of automated methods to measuring chromosomal damage.

Micronuclei (MN) formation in peripheral blood T-lymphocytes lends itself to automation, since the outcome of radiation damage is visually not too complex with limited variables. DNA damage incurred from ionizing radiation or chemical clastogens cause the formation of acentric chromosome fragments. The acentric chromosome fragments and whole chromosomes that are unable to engage with the mitotic spindle lag behind during anaphase (IAEA, 2011). Micronuclei originate from these acentric chromosome fragments or whole chromosomes which are excluded from the main nuclei during the metaphase/anaphase transition of mitosis. The lagging chromosome fragments or whole chromosomes form a small separate nucleus visible in the cytoplasm of cells.

Image recognition software can thus be more readily employed to quantify radiation damage. This requires the use of image classifiers that describe cell size, staining intensity, cell separation, aspect ratio and cell characteristics.

Rationale for This Study

The principal objective of this study was to define RBE variations for high-LET radiation with respect to radiosensitivity in human lymphocytes. Specifically this was done for very high energy neutrons and Auger electrons. The study was relevant as the relationship between neutron RBE and radiosensitivity of cells was unclear.

In general the response of different cell types varies much more to treatment with low-LET radiation compared to high-LET radiation (Broerse and Barendsen, 1973). Radiosensitivity differences have been demonstrated for different cancer cell lines (Slabbert *et al*., 1996) as well as various other clonogenic mammalian cells (Hall and Giaccia, 2005) exposed to both high and low-LET radiation. In general there is an expectation and in certain cases some experimental evidence to support less variations in radiosensitivities of cells to high-LET radiation. Furthermore the ranking

in the relative radiosensitivity of cell types differs for neutron treatments compared to exposure to X-rays (Broerse and Barendsen, 1973).

To quantify the radiation risk of individuals exposed to cosmic rays or mixed radiation fields of neutrons and γ-rays, several experiments were conducted to ascertain biological damage induced by neutron beams of various energies (Nolte *et al.*, 2007). Clonogenic survival data (Hall and Giaccia, 2005), dicentric chromosome aberrations (Heimers, 1999) and micronuclei formation (Slabbert et. al 2010) have been followed. Chromosome aberration frequencies have been quantified which allow estimation of radiation risk from neutrons with energies ranging from 36 keV up to 14.6 MeV (Schmid *et al.*, 2003). To complement these studies additional measurements have been made for blood cells exposed to 60 MeV (Nolte *et al.*, 2005) and 192 MeV (Nolte *et al.*, 2007) quasi monoenergetic neutron beams. Comparisons of RBE values obtained in these studies are shown in Fig. 1.8. Significant changes in the maximum relative biological effectiveness (RBE_M) of these neutron sources are demonstrated as a function of neutron energy, with a maximum value of 90 at 0.4 MeV. RBE_M drops to approximately 15 for neutron energies higher than 10 MeV and it appears that the RBE_M remains constant up to 200 MeV. The RBE_M values of 47 to113 reported by Heimers, (1999) are not consistent with these observations.

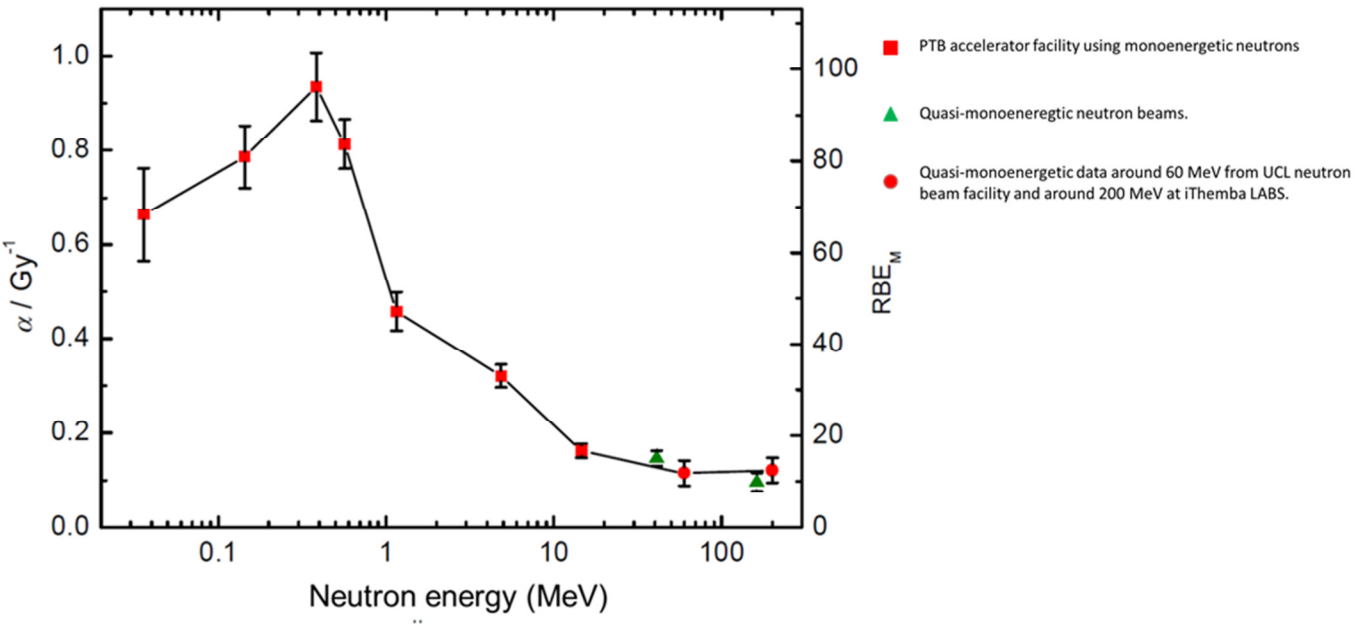

Figure 1.8: RBE_M values for neutrons of different energies (Nolte *et al.*, 2007).

The data shown in Fig. 1.8 was obtained by using the blood cells of a single donor. This was to ensure consistency in the biological response for different neutron energies used in different radiation facilities in different parts of the world. Keeping the donor constant has the advantage that only a single data set for the reference radiation was needed. These measurements were done over several years. In all these studies, dicentric chromosome aberrations were followed. As informative as these investigations may be, it is doubtful if RBE values obtained from blood samples from a single donor are indeed representative for the wider population to state radiation weighting factors.

It is unclear if RBE values for high energy neutrons will vary when measured with cells with different inherent radiosensitivities. Warenius *et al*. (1994) demonstrated that the RBE of a 62 MeV p+/Be neutron beam increases with an increase in radioresistance to 6 MV X-rays. Similarly Slabbert *et al.* (1996) using a p(66)/Be neutron with an average energy of 29 MeV, noted a statistically significant increase in the RBE values for cell types with increased radioresistance to ^{60}Co γ-rays. Although these investigators used 11 different cell types, few of these were indeed radioresistant to ^{60}Co γ-rays. Close inspection of the data shows that the relationship between neutron RBE and radioresistance to photons disappears when the cell type with the highest resistance to γ-rays (Gurney melanoma) is removed from the data set Slabbert *et al*. (1996).

In a follow up study the authors failed to demonstrate the relationship between RBE and radioresistance for a p(66)/Be neutron beam but such a relationship was demonstrated for a d(14)/Be neutron beam with a mean energy of 5.5 MeV (Slabbert *et al*., 2000). It therefore appears that the relationship for RBE and radioresistance is dependent on the selection of cells used in the study as well as the neutron energy.

Using lymphocytes Vral *et al*. (1994) demonstrated a clear reduction in RBE_M values for 5.5 MeV neutrons with an increase in the α-values of dose effect curves obtained for ^{60}Co γ-rays. This data was derived from lymphocytes obtained from six healthy donors. Using only four donors Slabbert *et al*. (2010) also demonstrated a relationship between RBE_M neutrons and radiosensitivity to ^{60}Co γ-rays. In the latter case the RBE_M values were found to be lower - as can be expected since these

investigators used a higher energy neutron source. Although a significant relationship between these parameters has been demonstrated by the investigators, the cohort of 4 donors in the study is very small. In fact 2 out of the 4 donors have different RBE_M values but appear to have the same radiosensitivity to ^{60}Co γ-rays.

A study employing a larger number of donors with blood cells exposed to high energy neutrons is clearly needed. It is particularly relevant to verify the findings above in order to indicate the correct w_R values for donors with different inherent radiosensitivity.

The studies of RBE variations with neutron energy by Schmid *et al*. (2003) and Nolte *et al*. (2005) were conducted by observing dicentric formations in metaphase spreads. This is an extremely labour intensive exercise. Indeed, it took more than six months to analyse the data for different doses for blood cells obtained from a single donor exposed to a single neutron energy and reference radiation. It follows that some method of automation is essential to assist the radiobiological evaluation of cellular radiation damage to quantify w_R values as a function of radiosensitivity.

Recently a semi-automated image analysis system has become available at iThemba LABS. This apparatus allows for semi-automated detection of micronucleus formations in irradiated cells. The main objective of this study is to ascertain the usefulness of this instrument to quantify micronuclei formations in large numbers of cells after exposure to high energy neutrons or ^{60}Co γ-rays. Of particular interest was to establish the minimum dose that such an automated process required firstly to distinguish MN formations from background readings secondly the accuracy in obtaining dose response curves that reflect both the quantitative and qualitative effects of the respective radiation modalities. This includes testing the ability of this image analysis method to accurately detect multiple MN formations in cells. The latter is reflected in dispersion parameters that are distinctly different for neutrons and ^{60}Co γ-rays. Also to establish if cytogenetic damage could be identified with sufficient accuracy to distinguish the inherent radiosensitivity of different donors. In addition it was important to know if RBE values as a function of dose obtained using this image analysis method was consistent with theoretical expectations.

An important aspect of this study is to establish if there is indeed a definitive correlation of the RBE_M values and inherent radioresistance of lymphocytes obtained from different individuals.

An additional objective of the study is to compare the variations in MN formations induced by an Auger electron emitter in lymphocytes to that of ^{60}Co γ-rays using blood from donors that were identified in the first part of the study as radiosensitive, radioresistant and an intermediate. It is important to ascertain the potential for therapeutic gain in oncology when treating cells with different inherent radiosensitivities using radionuclides that emit high-LET radiation.

Chapter 2

Materials and Methods

p(66)/Be Neutrons

Central to this study was the use of a high energy neutron beam, one of only two in the world currently used for neutron therapy. This beam was produced with a separated sector cyclotron (SSC) directing 66 MeV protons on to a beryllium (Be) target. The mean energy of the neutrons is 29 MeV (Jones *et al*. 1992). The beam is hardened as it passes through a hydrogenous filter that removes the low energy neutron component which has been shown to have a significant effect on the biological outcome in irradiated cells (Slabbert *et al*., 1989). Helpful in these experiments is the fact that the beam can be delivered at 0 degrees pointing downwards so that experimental cell samples placed on a treatment couch can easily be irradiated.

Cell samples were irradiated in test tubes placed on a 10 cm thick 30 x 30 cm stack of perspex used as back scatter material. Samples were covered by a 2 cm thick 30 x 30 cm nylon sheet that was used as build-up material. During the irradiations the dose rate was measured by monitoring the target current. This was kept at 15 µA which translates to a dose rate of 0.169 Gy/min depending on the setup and field size. A 29 x 29 cm field was used throughout the study. Using this setup the gamma dose component of this beam was 6.9 % (Slabbert *et al*. 1989).

Blood samples of different donors were irradiated on different days. Before each session dose output factors were measured to confirm dose delivery parameters monitored by a transition ionization chamber. These readings were done using a calibrated tissue equivalent ionization chamber.

^{60}Co γ-rays

A teletherapy unit (Theratron 780) was used to expose cells to ^{60}Co γ-rays. Cell samples were placed on a 0.5 cm thick 30 x 30 cm perspex table and a 10 cm thick 30 x 30 cm perspex block was placed on top of the cells to provide full scattering conditions. The beam points vertically upwards and has a source surface distance (SSD) of 75 cm. This setup has a dose rate of 0.5 Gy/min.

Calibration and dose verification on the Theratron ^{60}Co γ-ray teletherapy unit was performed with a NE farmer-type 0.6cc ionization chamber and matched electrometer. Measurements were performed in the same orientation and with the same setup parameters as described above for the cells.

Dose rate corrections were applied weekly during this study using a half-life of 5.272 years for ^{60}Co γ-rays. The dose rate applicable to the specific experiment A_T was calculated as:

$$A_T = A_0 e^{-\lambda t}$$

where $$t_{\frac{1}{2}} = \frac{\ln(2)}{\lambda}$$

A_T – dose rate at time T
A_0 - initial dose rate measured
λ - decay constant
t – time between date of measurement and experiment
$t_{½}$- half-life

Blood Sample Collection

This work was conducted with consent from the Health Research Ethics Committee (Ethics Reference #: S12/04/091). This procedure was performed by a registered healthcare worker in a hospital clinic: Blood samples were obtained from ten consenting adults of varying age (26 to 64). This includes 6 males and 4 females. Peripheral blood was collected aseptically by venipuncture into lithium heparin vacutainer tubes. From each donor ten tubes of 4.5 mℓ blood were collected. Immediately after collection the tubes were inverted carefully to mix blood and anti-coagulant. Blood samples where coded to safeguard subjects' identity and kept at room temperature (approximately 20˚C) for 1 hour before it was processed in the laboratory.

Lymphocyte Isolation

Although cultures of lymphocytes can be setup from whole-blood samples, lymphocytes were isolated in this study to ensure consistency in cell preparations to support automated image analysis. Cell numbers per samples were kept constant by pooling the isolated lymphocytes and dividing aliquots evenly between controls and samples irradiated at different doses and to different radiation qualities.

All cell preparation procedures were carried out in a biological safety cabinet. Lymphocytes were isolated from whole blood samples using a density gradient centrifugation method. For this whole blood was mixed in a ratio of 1:1 with Roswell Park memorial Institute (RPMI) 1640 tissue culture medium. From this 9 mℓ medium and blood mixture was carefully layered onto 3 mℓ Lymphocyte Separation Medium (LSM) in a 15 mℓ centrifuge tube.

Following centrifugation for 30 min at relative centrifugal force of 180 g the several layers of cells and serum were clearly visible. The erythrocytes accumulated at the bottom of the tube and a cloud of lymphocytes clustered in the plasma LSM interphase. The blood plasma layer was aspirated, without disturbing the cloud of lymphocytes. Lymphocytes were then collected with a 10 mℓ pipet. Excess platelets

and plasma was removed from this using a wash with phosphate buffered saline (PBS).

Lymphocytes pellets were pooled and resuspended in 10 mℓ RPMI 1640 medium supplemented with 15 % fetal calf serum and antibiotics. The concentration of cells in the stock suspension was determined with a Neubauer hemocytometer. From the lymphocyte stock 16 cell cultures per donor were prepared in test tubes that consisted of about $1x10^6$ cells in 5 mℓ growth medium.

External Beam Exposures

Test tubes containing cell cultures were placed in a water bath at 37˚C for 15 minutes prior to irradiations. The samples were irradiated with doses of 0.05, 0.1, 0.2, 0.5, 1, 2 Gy neutrons. Immediately after this additional samples from the same donor were exposed to doses of 0.05, 0.1, 0.2, 0.5, 1, 2, 4 Gy ^{60}Co γ-rays.

Cell Cultures

Following the completion of all the irradiations the mitogen Phytohaemagglutinin M-form (Sigma-Aldrich) was added to the cultures to a final concentration of 20 µg/mℓ. This stimulates T-lymphocytes into mitosis. Cultures were incubated at 37℃ and 5% CO_2. After 44 hours cytochalasin B (Sigma-Aldrich) was added to the cultures to a final concentration of 3 µg/mℓ. This inhibits cytokinesis and renders cells binucleated when allowed to grow for another 28 hours. After a total period of 72 hours cultures were terminated. Firstly cell suspensions were centrifuged at 180 g for 5 minutes. Then the supernatant was removed and 7 mℓ of 75 mM KCl was added. This hypotonic treatment renders cells in a swollen state to facilitate microscopic analysis. Samples were then centrifuged for 8 min at 180 g and the supernatant removed.

Cells were fixed in a two-step procedure. First by adding 5 mℓ of a 4:1:5 methanol: acetic acid: Ringer's solution. The ringer solution was made up by dissolving 6.5 g NaCl (Merck), 0.42 g KCl (Merck), 0.25 g $CaCl_2$ (Merck) in 1 ℓ deionized water. Cell suspensions were kept in the refrigerator at 2 ˚C overnight. The next day

suspensions were centrifuged at 180 g for 8 min and the supernatant was removed. Then 5 mℓ 4:1 methanol:acetic acid was added. This fixation procedure was repeated 3 times to ensure a cell preparation free of debris that can influence the automated detection and analysis of samples.

Four slides were made per culture by dropping 50 µℓ cell suspension on a clean microscope slide. Once the slides were dry, cells were stained by adding a drop of Vectashield DAPI (Vector Labs) before applying a 24 x 50 mm glass coverslip. Slides were kept in the dark for 1 hour before microscopic analysis.

Automated Detection of Cells and Scoring Of Micronuclei

Micronuclei (MN) formations in binucleated (BN) lymphocytes were enumerated semi-automatically by means of a software module developed by MetaSystems explicitly for the Metafer 4 platform. This consists of a Zeiss Axio Imager microscope equipped with a high-resolution charge coupled device (CCD) camera. The camera captures images of cells illuminated with an epi-florescence filter set with an excitation wave length of 358 nm and emission wavelength of 461 nm. With this cell nuclei have a characteristic blue fluorescence. The software drives a Märzhäuser motorized microscope stage that accommodates 8 microscope slides at a time.

This system automatically identifies BN cells that meet programmed criteria defined by a set of image classifiers. Cells are only scored as binucleates if the main nuclei are of approximately equal size and shape.

A second classifier is applied to all the identified BN cells. This classifier numerates MN frequency in the BN cells. To qualify as a MN the diameter of the MN should be less than one-third of the main nucleus. Also MN should be separated from the main nuclei and the MN should have similar staining characteristics' as the main nucleus. The software interphase, displays the total number of BN cells, the MN frequency distribution histogram and a screen gallery of cell images (Fig. 2.1).

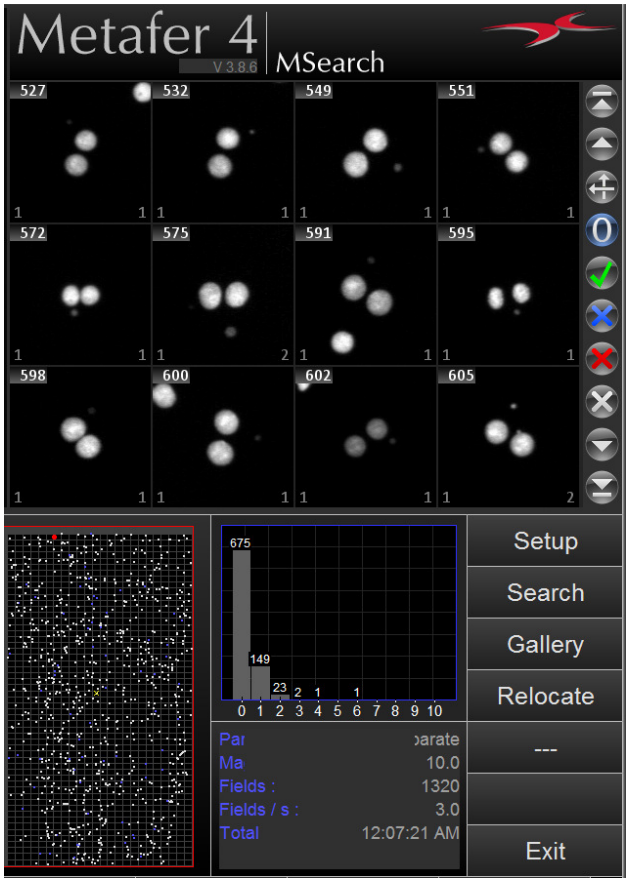

Figure 2.1: Metafer4 software interface display for MN analysis.

The system was set up to detect 1000 BN per slide on a predefined area covering about 90 % of the microscope slide. Before the scanning of slides can take place an initial focus point needs to be set manually on each of the 8 slides on the motorized stage. Following this the system automatically identifies several grid focus points on the slide to enable faster scanning of cell images on each slide.

Poor image quality of some samples resulted in less than 1000 BN cells identified per slide. Of the four slides prepared per culture, the 2 slides with the highest cell counts were used in the analysis. In this a minimum of 500 BN cells were counted per slide. Thus a minimum of 1000 cells per sample were analyzed for MN formations.

The images were backed up on a hard drive. The classifiers for the identification of BN and MN were based on the criteria developed in a previous collaborative study between iThemba LABS and the University Ghent, Belgium (Willems *et al*. 2009).

These sets of classifiers were optimized for detecting BN cells and enumerating MN in slides prepared from whole-blood cultures. Minimal adjustments to the parameters displayed below were made to optimize the classifier for scanning cell samples prepared from isolated lymphocytes.

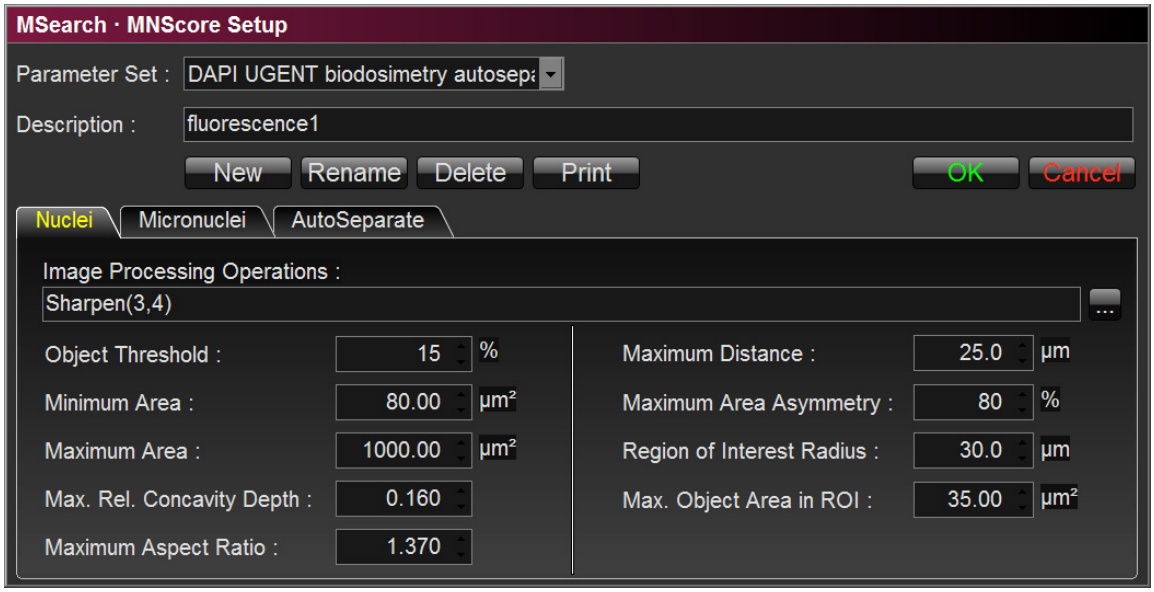

Figure 2.3: Classifier parameters describing the constraints imposed on BN cells' selection.

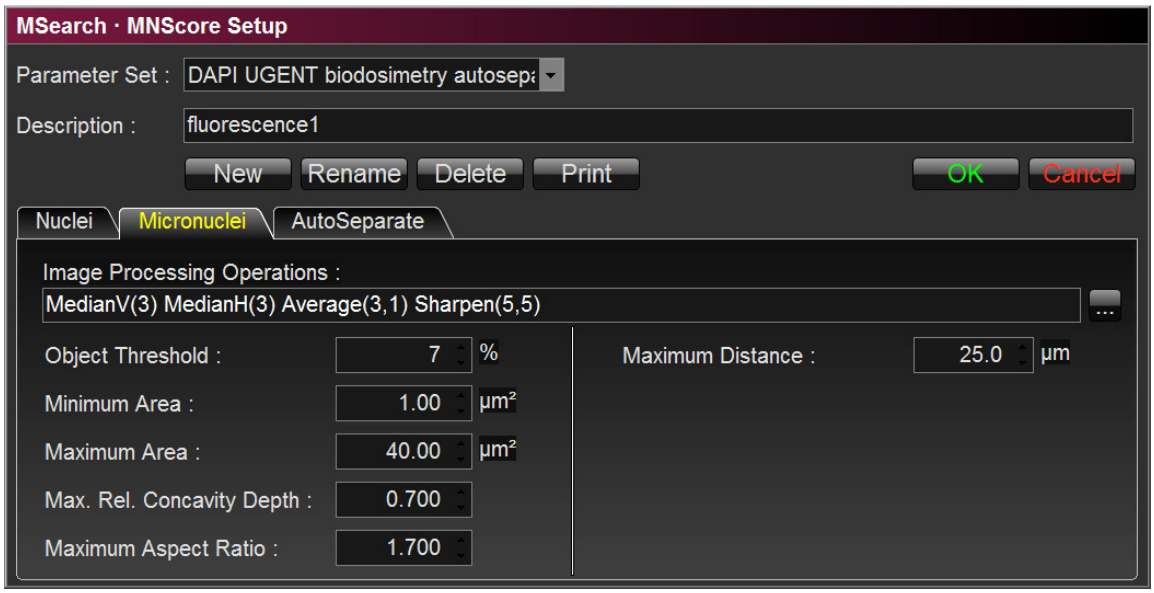

Figure 2.4: Classifier parameters describing the constraints imposed on MN selection.

Manual Verification of Cellular Radiation Damage

Following each scan, cells identified by the classifier that contain MN were manually inspected. Visual scrutiny of the MN formations was done to verify the number of MN noted per cell. This was done to exclude false positive MN that resulted from debris or image aberrations.

Statistical Analysis

Dose Response Curve

The biological responses to a wide range of doses were investigated for different treatment modalities and for different donors. To estimate the dose response parameters as accurately as possible the experimental design included data for several low dose treatments as well as high doses. MN frequencies (MNF) defined as the number of MN observed in 1000 BN cells were related to the radiation dose as follows.

$$MNF = c + \propto D + \beta D^2$$

where:

MNF – Number of MN per 1000 BN cells

D – Dose (Gy)

c – Spontaneous background MN count

α and β - Represent the initial slope and bending component of each dose response curve. These values reflect the inherent radiosensitivity and the capacity of cells to accumulate repairable damage respectively.

GraphPad prism 4 was used to plot the dose response curves and to perform non-linear regression analysis. In cases where the β-component did not significantly differ from zero, the value was set to 0 and the α-parameter recalculated. The package was also used to calculate the mean and standard deviation (SD) of the different data sets.

95 % Confidence Ellipses

In addition a computer program has been developed on a Matlab platform to perform advanced statistical analysis. Essentially this program calculates the 95 % confidence ellipse for the co-variance parameters α and β that describe the dose response curve. The program is based on the method used by Slabbert *et al*. (1989). This is needed to ascertain if the differences in radiosensitivity of different donors can be stated on the 95 % confidence level. The probability of induction of intra-track cellular radiation damage – reflected by the α-value is co-variant to the induction of inter-track damage reflected by the β-value. When α is large, β becomes smaller. The computer program calculates an ellipse region around a coordinate that is defined by the mean estimate of the α-value - plotted on the X-axis and the β - value plotted on the Y-axis. The inherent radiosensitivity of lymphocytes obtained from various donors differs on a 95 % confidence level, only when the ellipses do not overlap. An overlapping region indicates that the same α and β value can be used to describe dose response relationships for different donors. Donors were ranked in terms of their radiosensitivity to ^{60}Co γ-rays. For this radiation modality all least square estimates of the respective β values were positive. Negative β values were calculated only for some dose response curves to high-LET radiation. The dose response curves resembled straight lines due to the small β values with increasing uncertainties. Therefore should the negative β values be set to zero for all the neutron ellipses, more overlapping between ellipses of data for different donors will occur. This advances the argument that variation in radiosensitivity amongst the different donors diminishes with increased LET. Variation in the inherent radiosensitivity amongst the donors is thus best expressed using responses to low-LET radiation.

Dispersion Parameters

In this study it is important to understand both the quantitative and qualitative responses to neutrons and γ-rays. Assuming a Poisson distribution applies to the induction of MN it can be expected that the ratio of the variance (σ^2) to the mean ($\bar{y}$) should be a value of 1 (Huber *et al*. 1992). The numerical package Mathcad 15 was used to estimate the dispersion parameters for MN inductions as follows:

$$\frac{\sigma^2}{\bar{y}} = \frac{\sum_{l=1}^{N_i}(k_i - \bar{y})^2}{(N_i - 1)}$$

where k_i is the number of MN in the l^{th} of N cells $\bar{y}$ is the mean MN frequency (Huber *et al*. 1992).

To determine whether the mean and the variance of the observed distributions were significantly different, the standard normal deviate of $\sigma^2/\bar{y}$ was calculated according to Savage (1970):

$$\mu = \frac{d - (N-1)}{\sqrt{2(N-1)(1 - \frac{1}{N\bar{y}})}}$$

where $$d = (N-1)\frac{\sigma^2}{\bar{y}}$$

A positive value of μ indicates an over-dispersion of MN and negative value under-dispersion compared to that expected from a Poisson distribution. If the μ-value of is larger than 1.96, the under-or-over dispersion is significant on a 95 % confidence level.

Chapter 3

Results

Cell Cultures

It is essential that the cell cultures set up for these experiments could be successfully stimulated from normal non-dividing lymphocytes into mitosis and to arrest them in a state of binucleation. The cell culture kinetics for the different donors is listed in Table 3.1.

Table 3.1: Cell culture kinetics for unirradiated lymphocyte cultures from 10 different donors.

	1 Nucleus	2 Nuclei	3 Nuclei	4 Nuclei	Gender	Nucleation index	Percentage BN
Donor 1	49	43	6	2	Male	1.61	47
Donor 2	68	28	4	0	Female	1.36	29
Donor 3	55	41	4	1	Male	1.53	43
Donor 4	37	53	9	0	Male	1.70	59
Donor 5	63	33	5	0	Female	1.44	34
Donor 6	65	32	3	0	Male	1.38	33
Donor 7	76	23	1	0	Female	1.25	23
Donor 8	56	40	3	1	Male	1.49	42
Donor 9	68	26	3	3	Female	1.41	28
Donor 10	55	39	3	1	Male	1.46	41

The cell culture kinetics were shown as the percentage of cells observed to have 2 nuclei (binucleated cells) as well as a nucleation index calculated for the cultures control cells that received no radiation. The nucleation index was indicated as the total number of main nuclei noted in the total number of cells analysed. The

percentage binucleated cells (BNC) ranged from 23 % to 59 % and nucleation indices ranged from 1.25 to 1.61. It was interesting to note that blood collected from females resulted more frequently in poorer stimulations compared to that collected from male donors. This has periodically been noted by investigators using lymphocyte cultures.

All the cultures set up in this study proved to be successful to produce sufficient number of BNC's that could be used to prepare microscopic slides for MN analysis.

Dose Response Curves

Background Readings

MN observed in non-irradiated cell cultures ranged from 4 to 15 MN per 1000 BNC's for the different donors. Differences in spontaneous MN formation were correlated to donors' gender. The mean spontaneous MN frequency for male donors was 7 ± 0.8 whilst that for females was 12 ± 2.1. On average the background MN frequency was almost double that for male donors and the difference is statistically significant (p-value 0.0343).

Radiation Induced MN

The minimum dose where radiation induced MN could be distinguished from background readings for all donors was 200 mGy γ-rays. At 100 mGy MN frequencies for 7 donors were higher than that of their respective control samples. For 6 donors the MN frequency observed for a dose of 50 mGy was in fact larger than the back ground readings, although not significantly.

Clear dose response curves could be established for all donors in this study for blood cells irradiated with either neutron or γ-rays (Fig. 3.1). The neutron and γ-ray induced MN formations were clearly different in each instance. Out of the 160 dose points analysed in this study only one neutron dose point recorded for donor 7 was not consistent with this observation.

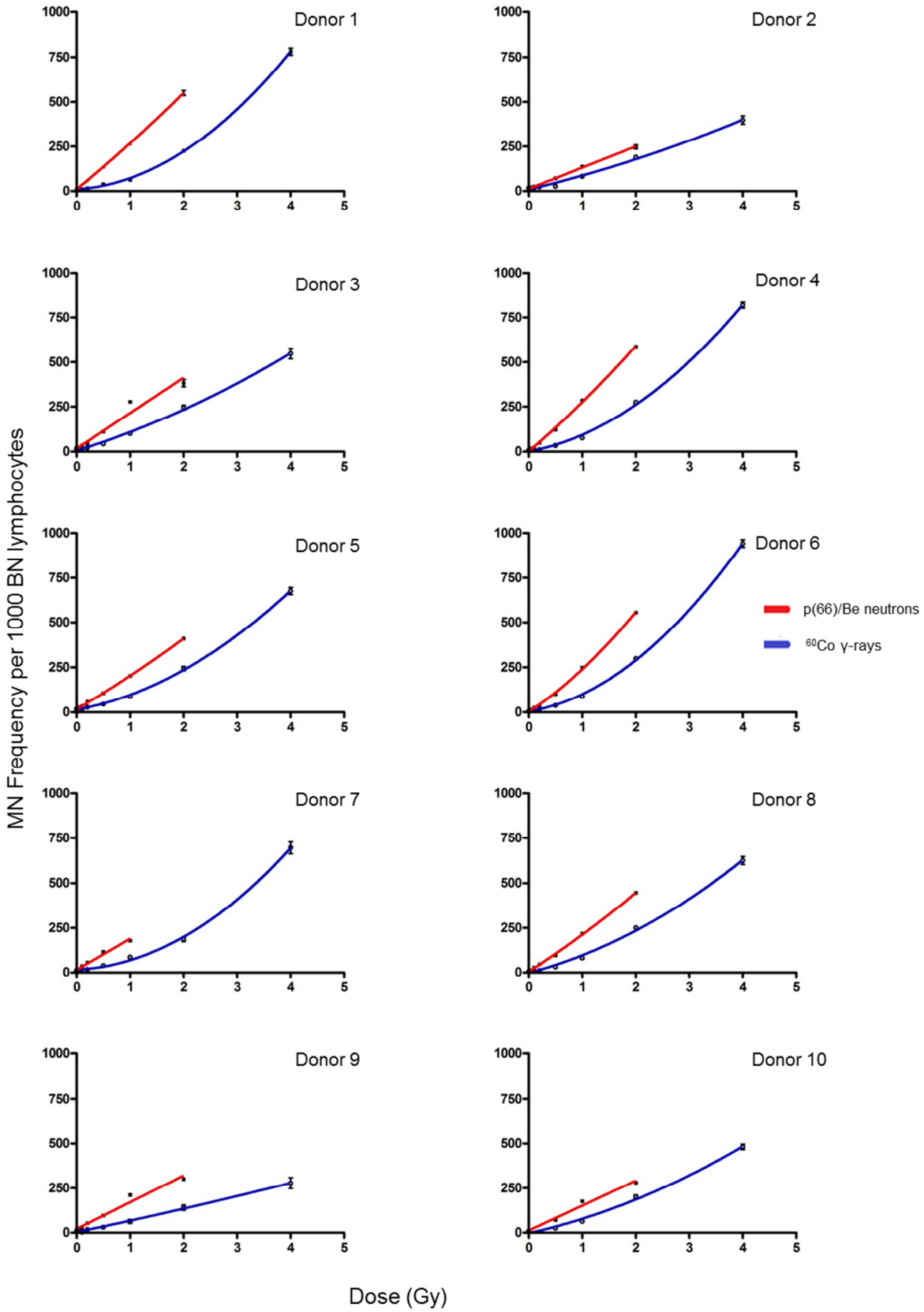

Figure 3.1: Dose response curves for MN formations in isolated T-lymphocytes of 10 different donors after exposure to various doses of ^{60}Co γ-rays or p(66)/Be neutrons. The Poisson error is indicated in each instance.

The shapes of the response curves for the different donors were not the same. In general a clear linear-quadratic relationship was noted for γ-rays and a more linear response with dose was prominent for neutrons. The fitted dose response parameters are listed in Table 3.2.

Table 3.2: Dose response parameters for lymphocytes irradiated with different doses of neutrons or γ-rays.

Donor ID	^{60}Co γ-rays		p(66)/Be neutrons	
	α (Gy^{-1})	β (Gy^{-2})	α (Gy^{-1})	β (Gy^{-2})
Donor 1	19.39 ± 5.7	43.4 ±1.4	251.1 ±4.9	3.1 ±2.4
Donor 2	71.45 ± 11.7	6.6 ±2.9	118.7 ±10.0	0 0
Donor 3	91.13 ± 10.2	11.2 ±2.6	197.9 ±75.9	0 0
Donor 4	54.06 ± 10.9	37.8 ±2.7	255.3 ±17.8	19.6 ±8.8
Donor 5	54.38 ± 7.1	27.8 ±1.7	175.5 ±7.4	10.1 ±3.6
Donor 6	49.81 ± 7.6	46.3 ±1.9	195.6 ±17.2	40.7 ±8.5
Donor 7	13.84 ± 10.8	38.8 ±2.7	174.1 ±61.2	0 0
Donor 8	79.05 ± 12.4	19.6 ±3.1	193.3 ±11.9	13.6 ±5.8
Donor 9	62.33 ± 5.7	1.6 ±1.4	149.3 ±50.2	0 0
Donor 10	66.84 ± 22.2	13.7 ±5.2	139.5 ±71.0	0 0

The initial slopes represented by the α-values for all γ-irradiated dose response curves were larger than zero. This notwithstanding the fact that the minimum dose of 50 mGy used in this study induced MN formations less than the respective background. The latter was included in the curve fitting procedure. α-values varied from 13.8 Gy^{-1} to 91.1 Gy^{-1} with a mean value of 56.2 Gy^{-1}. The quadratic component β-value was also larger than zero in all samples. β-values between 1.6 Gy^{-2} and 46.2 Gy^{-2} are noted with a mean value of 24.7 Gy^{-2}.

For neutron irradiations larger α-values than that seen for γ-rays were observed for all samples. It was noted that the standard error in some instances is relatively large in particular in the case of Donor 7, who also exhibited a large uncertainty in the γ-dose response curve.

Unlike the γ-dose response curves, the β-component for neutron irradiations was not larger than zero. The β-value for 5 of the 10 neutron dose response curves proved to be not significantly different than zero.

Although the dose response parameters for the different donors varied in magnitude, any changes in the inherent radiosensitivity of the different donors could only be ascertained once the uncertainties around the α- and β-values were analysed correctively. For this reason 95 % confidence ellipses have been constructed for lymphocytes irradiated with γ-rays (Fig. 3.2).

Radiosensitivity Specifications of Lymphocytes from Different Donors Exposed to ^{60}Co γ-rays and Neutrons Using 95 % Confidence Ellipses

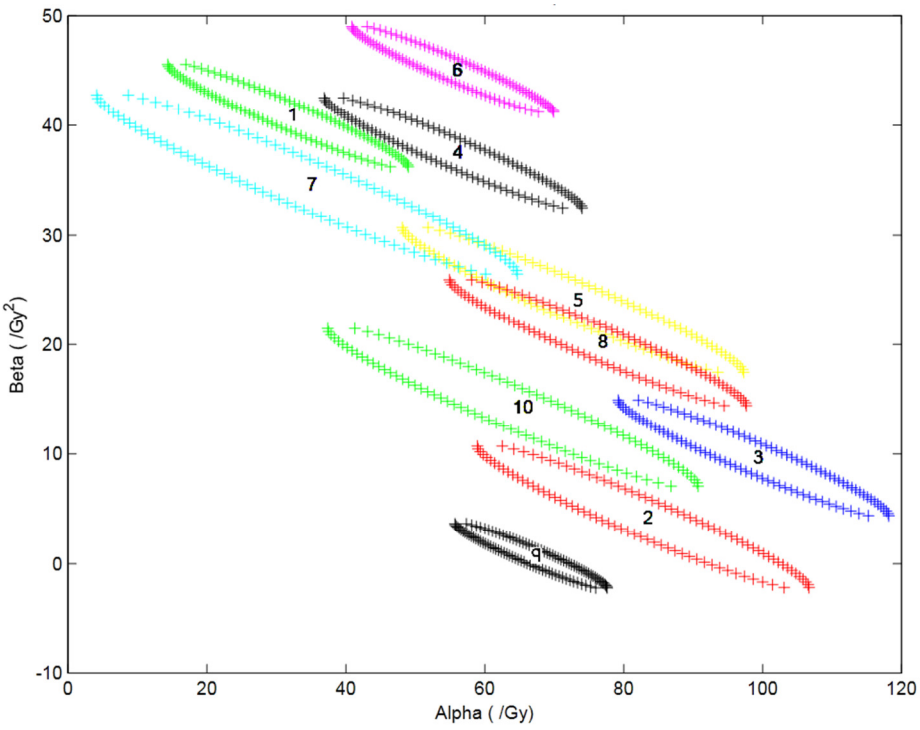

Figure 3.2: The 95 % confidence ellipses for dose response parameters for lymphocyte samples of different individuals irradiated with ^{60}Co γ-rays.

Variations in the inherent radiosensitivities of lymphocytes of donors to γ-rays could be stated to be statistically significant at the 95% level of confidence for most donors.

The confidence ellipses around the mean α- and β-value estimated in each instance were separate. The only exception was the MN formations for donors 5 and 7 and 5 and 8. For these individuals an overlap of the confidence ellipses were noted. This represents a common set of α-and β-values that could be used to describe both dose response curves.

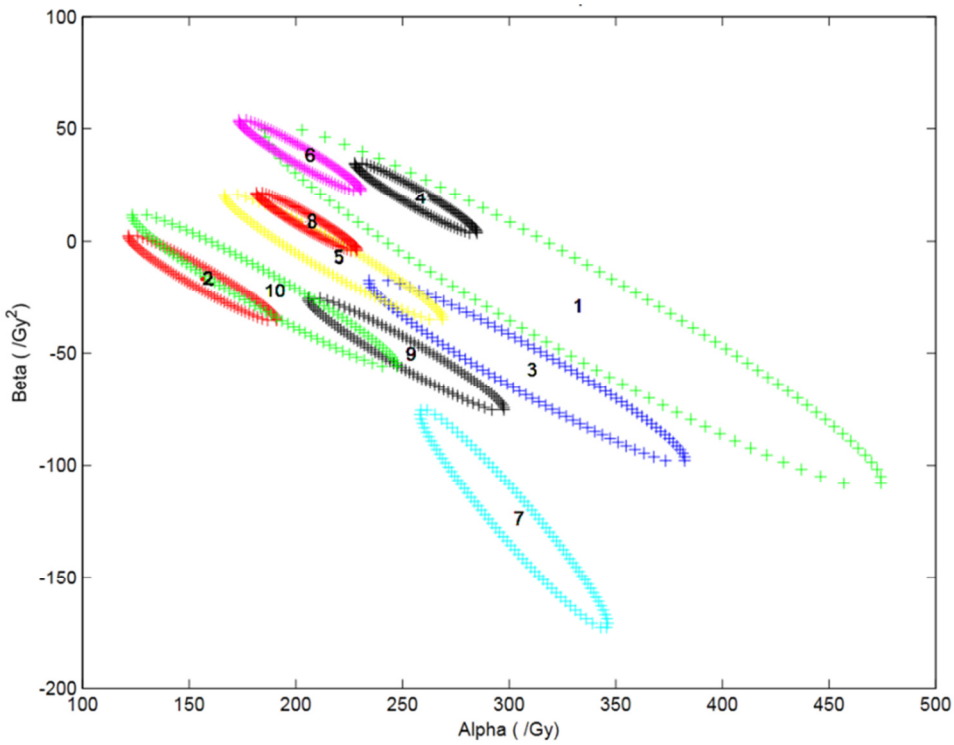

Figure 3.3: The 95 % confidence ellipses for dose response parameters for lymphocyte samples of different individuals irradiated with p(66)/Be neutrons.

Variations in the inherent radiosensitivities of lymphocytes of donors to neutrons were significantly different to that seen for γ-rays. The confidence ellipses for neutrons were generally larger than those observed for γ-rays (Fig. 3.3). The size difference was in part due to the fact that the physical dose range over which the dose response curves were constructed was smaller for neutrons (0 - 2 Gy) compared to γ-rays (0 - 4 Gy). As a result larger variations in the estimation of α-and β-values were noted. Even so many overlaps of the confidence ellipses for lymphocytes treated with neutrons could be seen for the different donors. Only the response of lymphocytes from donor 7 to neutrons was uniquely different from the rest. Even so, statistical significant differences in the response to high energy

neutrons for lymphocytes of some donors could be stated with respect to that of others. For example the confidence ellipse for donor 9 was significantly different from donors 2 and 8 but not from donor 10. In general a reduced variation in the radiosensitivities to neutrons for lymphocytes of different donors was evident.

The 10 donors were ranked in terms of their radiosensitivities noted for lymphocytes exposed to ^{60}Co γ-rays. Their corresponding radiosensitivity rank observed following exposure to neutrons is shown in red (Fig. 3.4). Notable differences in the ranking of different individuals exposed to two different radiation modalities are noted. Donors sensitive to ^{60}Co γ-rays were assumed to be equally sensitive to neutrons. This is however not the case, as the increase in relative neutron sensitivity exhibits no correlation to the increase in relative sensitivity to ^{60}Co γ-rays.

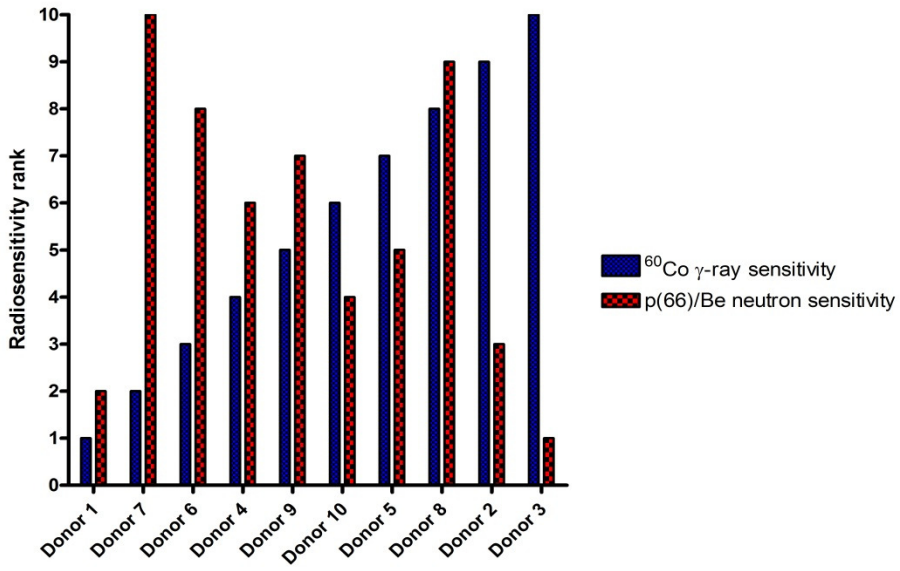

Figure 3.4: Subjects ranked in terms of radiosensitivity to ^{60}Co γ-rays with their corresponding radiosensitivity rank to p(66)/Be neutrons displayed in red (10 = most sensitive and 1 = most resistant).

Dispersion Parameters

Parameters that describe the distribution of MN in the irradiated cell population were required for several reasons. The number of cells containing 0, 1, 2 up to 8 MN per cell was a reflection of the ionization density of the radiation used in the experiments.

Of interest in this study was to establish if the semi-automated image analysis method used in evaluating cellular radiation damage, was able to detect a distribution pattern of MN formations that is consistent with expectations.

Using the numerical methods described in the previous chapter, the dispersion index $\sigma^2/\bar{y}$ and the standard normal deviate, μ-value was calculated for each cell sample analysed. These are listed in Table 3.3 for ^{60}Co γ-rays and Table 3.4 for neutrons. A Poisson distribution was expected for MN observed in control samples where the ratio of $\sigma^2/\bar{y}$ should have a value of 1. Under-dispersion was noted for 4 out of the 10 background readings made in this study - $\sigma^2/\bar{y} < 1$ where μ is a negative number. The mean dispersion index for all the control samples was 1.06 and the readings noted were expected.

For cell samples irradiated with ^{60}Co γ-rays a Poisson distribution of cytogenetic damage was expected (IAEA, 2011). The number of MN observed per cell ranged from 0 to 8. Even so relative few samples displayed under-dispersion. Statistically significant ($\mu > 1.96$) over-dispersed distributions were noted in most readings. A mean value for dispersion indices of 1.12 was determined for all cell samples exposed to ^{60}Co γ-rays. The corresponding μ-value was 3.92. An unexpected small over-dispersion was noted for MN, which could be the result of observing this type of cytogenetic effect in BN cells.

Lymphocytes exposed to neutrons consistently yield MN formations with a larger dispersion index for each donor. The range of MN induced per cell was from 0 to 6. The maximum number noted was less than that for γ-rays but it was for neutron doses resulting in lower MN frequencies on average. Statistically significant over-dispersions were noted for all cell samples exposed to neutrons with a mean value of 1.19 and a corresponding μ-value of 7.05. The increase in these dispersion parameters have previously been consistent with cytogenetic damage observed in other studies (IAEA, 2011). These investigators indicated dispersion parameters of 1 for γ-rays compared to 1.19 for alpha particles with corresponding mean μ-values of 0.32 and 1.54 respectively.

By observing MN by eye different dispersion parameters has previously been noted for ^{60}Co γ-rays and p(66)/Be neutrons at iThemba LABS (unpublished data). In these studies average $\sigma^2/\bar{y}$ values of 1.04 were noted for γ-rays with a μ-value of 1.08. For neutrons these values increased to 1.15 and 2.62 respectively. When the build-up from neutron irradiations was removed, the secondary charged particles depositing dose is made up predominantly of short range alpha particles and heavy recoil fragments. Under these irradiation conditions, the $\sigma^2/\bar{y}$ value for MN formations in lymphocytes increased to 1.30 and a μ-value of 6.25 was observed. Comparing the results of the current study with these values it is clear that the semi-automated image analysis system was indeed able to detect MN formations in irradiated cells with a distribution pattern that reflects the qualitative characteristics of the radiation modality. This was summarized in Fig. 3.5 showing the mean distribution parameters for the different donors.

Table 3.3: The dispersion parameters describing the distribution of MN in the ^{60}Co γ-ray irradiated lymphocyte samples.

			Number of cells observed with n number of MN										
Dose	Total MN	Total BN	n=0	n=1	n=2	n=3	n=4	n=5	n=6	n=7	n=8	$\sigma^2/\bar{y}$	μ-value
Donor 1													
0	30	3794	3765	28	1							1.06	2.5
0.05	38	3762	3728	31	2	1						1.25	11.0
0.1	31	2561	2531	29	1							1.05	1.9
0.2	61	3708	3653	50	4	1						1.21	9.2
0.5	125	3215	3095	116	3	1						1.06	2.3
1	217	3398	3203	174	20	1						1.15	6.1
2	743	3296	2677	509	98	10	2					1.13	5.3
4	1602	2049	1087	523	294	100	37	6	1	1	1	1.39	12.5
Donor 2													
0	49	2944	2901	40	2			1				1.08	2.5
0.05	51	2827	2781	42	3	1						1.35	13.3
0.1	68	3562	3499	58	5							1.13	5.4
0.2	55	2404	2354	45	5							1.16	5.5
0.5	70	2652	2588	59	4	1						1.17	6.3
1	220	2661	2466	173	19	3						1.17	6.3
2	509	2678	2255	348	66	7	2					1.20	7.3
4	298	749	549	131	43	23	3					1.48	9.2
Donor 3													
0	31	1843	1819	19	3	2						1.09	4.0
0.05	53	3059	3016	36	5	1	1					1.51	20.0
0.1	43	3478	3439	36	2	1						1.22	9.2
0.2	37	1897	1870	24	1	1				1		2.71	52.7
0.5	126	2892	2770	118	4							1.02	0.8
1	151	1503	1363	130	9	1						1.06	1.6
2	309	1263	1005	213	39	6						1.13	3.1
4	350	639	413	129	71	25	1					1.32	5.8
Donor 4													
0	29	3933	3905	27	1							0.99	-0.3
0.05	25	3859	3835	23	1							1.07	3.2
0.1	41	3774	3736	35	3							1.13	5.9
0.2	36	3702	3666	36								0.99	-0.4
0.5	127	3774	3652	117	5							1.05	2.0
1	287	3788	3517	256	14	1						1.04	1.9
2	773	2806	2148	552	97	9						1.05	1.7
4	2471	3014	1454	892	478	147	33	10				1.16	6.4

*Table 3.3 continues on next page

Dose	Total MN	Total BN	Number of cells observed with n number of MN									$\sigma^2/\bar{y}$	μ-value
			n=0	n=1	n=2	n=3	n=4	n=5	n=6	n=7	n=8		
Donor 5													
0	66	3724	3665	53	5	1						1.13	5.7
0.05	90	3768	3691	66	9	2						1.31	13.4
0.1	49	3335	3288	46	0	1						1.11	4.4
0.2	75	2652	2585	61	4	2						1.24	8.7
0.5	153	3421	3280	131	8	2						1.14	5.7
1	272	3086	2851	204	27	3	0	1				1.25	9.8
2	422	1739	1379	305	50	4	0	1				1.10	2.9
4	1132	1674	960	411	212	70	19	1	1			1.32	9.1
Donor 6													
0	12	2823	2811	12								1.00	-0.1
0.05	36	3714	3679	34	1							1.05	2.0
0.1	44	3491	3449	40	2							1.08	3.3
0.2	63	3589	3528	59	2							1.05	2.0
0.5	143	3756	3619	132	4	1						1.06	2.6
1	331	3767	3458	288	20	1						1.05	2.2
2	1070	3577	2682	737	143	13	2					1.06	2.7
4	1950	2069	920	599	357	146	38	7	2			1.21	6.8
Donor 7													
0	39	3322	3290	26	5	1						1.20	8.0
0.05	49	3790	3745	41	4							1.15	6.6
0.1	55	2929	2876	51	2							1.05	2.1
0.2	35	1996	1963	31	2							1.10	3.1
0.5	132	3417	3290	122	5							1.04	1.5
1	113	1307	1201	99	7							1.04	1.0
2	236	1279	1079	167	30	3						1.23	5.8
4	449	645	364	160	81	34	5	1				1.30	5.4
Donor 8													
0	22	3616	3595	20	1							1.00	-0.2
0.05	27	3782	3755	27								0.99	-3.0
0.1	34	3838	3807	28	3							1.16	7.4
0.2	40	3760	3722	36	2							1.09	3.9
0.5	119	3817	3702	111	4							1.04	1.6
1	201	2493	2305	177	10		1					1.02	0.7
2	810	3222	2542	570	96	11	1	1	1			1.07	2.7
4	792	1267	746	320	145	44	10	2				1.28	6.7

*Table 3.3 continues on next page

Dose	Total MN	Total BN	Number of cells observed with n number of MN									$\sigma^2/\bar{y}$	μ-value
			n=0	n=1	n=2	n=3	n=4	n=5	n=6	n=7	n=8		
Donor 9													
0	22	2638	2617	20	1							1.08	3.0
0.05	11	881	870	11								0.99	-0.2
0.1	1	300	299	1								1.00	0.0
0.2	36	2180	2144	36								0.98	-0.5
0.5	63	2056	1996	57	3							1.07	2.1
1	35	555	523	29	3							1.11	1.8
2	82	586	510	70	6							1.01	0.1
4	86	309	255	30	18	5		1				1.73	9.0
Donor10													
0	18	1978	1960	18								0.99	-0.2
0.5	50	1993	1949	40	3		1					1.33	10.6
1	131	1992	1878	105	7	2						1.09	2.9
2	402	1996	1661	272	60	2	1					1.16	5.0
4	959	1992	1403	317	191	64	17					1.53	16.8

Table 3.4: The dispersion parameters describing the distribution of MN in the neutron irradiated lymphocyte samples.

Dose	Total MN	Total BN	Number of cells observed with *n* number of MN							$\sigma^2/\bar{y}$	μ-value
			n=0	n=1	n=2	n=3	n=4	n=5	n=6		
Donor 1											
0	28	3777	3752	22	3					1.06	2.6
0.05	91	3884	3803	75	4	1		1		1.35	15.4
0.2	241	3878	3665	188	22	3				1.20	8.6
0.5	391	2866	2528	294	36	7	1			1.19	7.0
1	982	3678	2900	614	127	35	1	1		1.24	10.2
2	1632	2968	1853	733	276	80	23	3		1.29	11.1
Donor 2											
0	21	1824	1804	19	1					1.08	2.5
0.05	79	3706	3637	61	7		1			1.31	13.3
0.1	88	3538	3456	76	6					1.11	4.7
0.2	80	2552	2482	60	10					1.22	7.8
0.5	263	3663	3436	197	24	6				1.25	10.6
1	372	2692	2358	301	29	3	1			1.10	3.6
2	460	1861	1503	270	76	10	2			1.27	8.1
Donor 3											
0	39	3747	3710	35	2					1.09	4.0
0.05	69	3785	3721	59	5					1.13	5.5
0.1	127	3772	3660	98	13	1				1.22	9.5
0.2	149	3362	3228	123	8	2	1			1.22	9.2
0.5	305	2760	2499	225	29	6	1			1.24	8.8
1	879	3173	2476	546	126	20	4	1		1.22	8.9
2	354	927	676	170	61	18	2			1.30	6.5
Donor 4											
0	23	3834	3811	23						0.99	-0.3
0.05	66	3779	3721	51	6	1				1.26	11.1
0.1	82	3609	3533	70	6					1.12	5.3
0.2	164	3318	3179	118	17	4				1.30	12.4
0.5	457	3738	3329	369	36	2	1		1	1.15	6.6
1	972	3411	2630	627	124	23	7			1.20	8.2
2	1267	2153	1290	568	220	47	23	4	1	1.29	9.4
Donor 5											
0	54	3689	3639	46	4					1.13	5.7
0.05	95	3761	3680	69	10	2				1.31	13.5
0.1	94	2787	2703	77	5	1	1			1.27	9.9
0.2	215	3671	3489	155	22	4	1			1.31	13.5
0.5	93	877	802	61	11	2	1			1.39	8.2
1	506	2511	2103	325	69	13	1			1.12	8.8
2	1216	2971	2110	581	217	52	10	1		1.32	12.3

*Table 3.4 continues on next page

Dose	Total MN	Total BN	Number of cells observed with *n* number of MN							$\sigma^2/\bar{y}$	μ-value
			n=0	n=1	n=2	n=3	n=4	n=5	n=6		
Donor 6											
0	23	3440	3418	21	1					1.00	-0.1
0.05	59	3844	3789	51	4					1.12	5.3
0.1	97	3813	3722	85	6					1.10	4.3
0.2	139	3822	3698	109	15					1.18	7.9
0.5	385	3796	3455	300	38	3				1.14	6.2
1	808	3263	2612	520	106	24	1			1.21	8.4
2	1558	2809	1722	723	277	69	16	2		1.22	8.1
Donor 7											
0	19	3061	3044	15	2					1.20	8.0
0.05	33	2058	2025	33						0.98	-0.5
0.1	85	2283	2204	74	4	1				1.13	4.3
0.2	156	2745	2616	106	20	2	1			1.35	13.1
0.5	367	3173	2840	302	28	3				1.09	3.4
1	535	2981	2542	355	73	10	1			1.22	8.8
2	306	1506	1263	193	39	9	2			1.31	8.4
Donor 8											
0	16	3876	3860	16						1.00	-0.2
0.05	53	3800	3749	49	2					1.06	2.7
0.1	107	3828	3733	84	10	1				1.22	9.4
0.2	175	3799	3645	135	17	2				1.22	9.5
0.5	355	3712	3397	278	34	3				1.15	6.3
1	790	3643	2999	524	98	18	4			1.23	9.8
2	1361	3059	2081	683	225	54	14	2		1.28	10.8
Donor 9											
0	19	1301	1283	17	1					1.09	2.3
0.05	17	792	775	17						0.98	-0.4
0.1	19	739	722	15	2					1.19	3.6
0.2	67	1247	1187	53	7					1.16	3.9
0.5	109	1134	1038	83	13					1.14	3.4
1	72	341	288	39	10	3	1			1.49	6.4
2	281	937	748	126	43	14	4	1	1	1.66	14.2
Donor 10											
0	15	1991	1976	15						0.99	-0.2
0.2	74	1990	1923	60	7					1.15	4.8
0.5	141	1990	1873	97	18	1		1		1.37	11.7
1	409	1994	1701	245	40	7	1			1.04	1.2
2	560	1997	1555	340	88	13		1		1.21	6.6

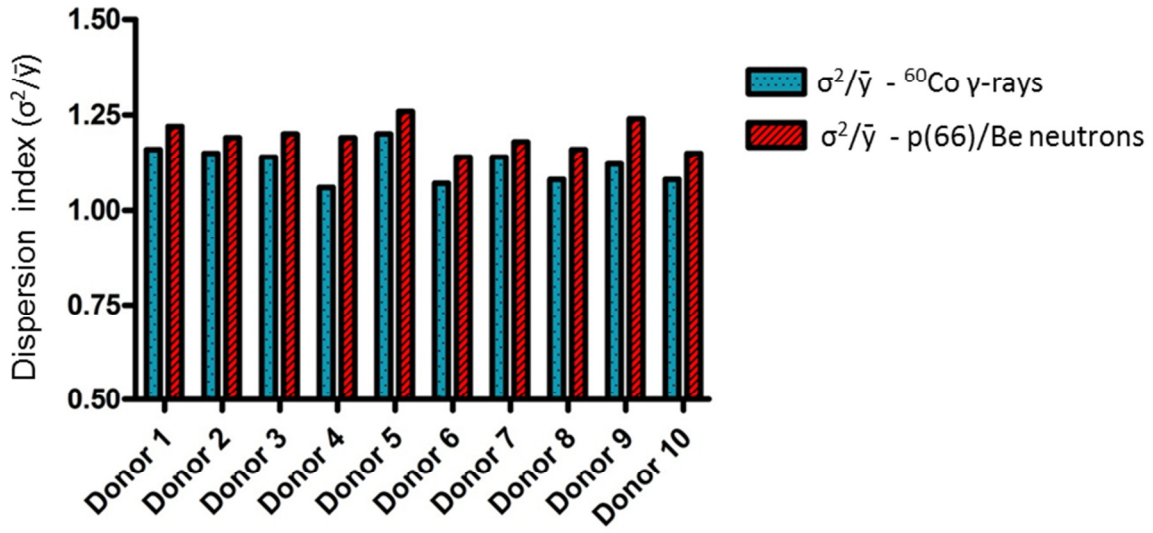

Figure 3.5: Comparison of mean dispersion indices ($\sigma^2/\bar{y}$) for the number of cells observed with N number of MN for cells exposed to ^{60}Co γ-rays and p(66)/Be neutrons.

Relative Biological Effectiveness

The principal interest in this study was to establish if a correlation exists between the neutron RBE and the inherent radiosensitivity of lymphocytes obtained from different donors. Significant variations in radiosensitivity to γ-rays - by a factor of 7 - established at a 95% confidence level (Fig. 3.2), allowed one to test for an increase in RBE with a decrease in radiosensitivity.

The dose limiting RBE values observed in lymphocytes of different donors were calculated as follows:

$$RBE_M = \frac{\alpha_{\ neutrons}\ (Gy^{-1})}{\alpha_{^{60}Co\ \gamma-rays}\ (Gy^{-1})}$$

where $\alpha_{neutrons}$ (Gy^{-1}) represents the initial slope of the dose response curve for p(66)/Be neutrons and $\alpha_{\gamma\text{-rays}}$ (Gy^{-1}) represents the initial slope of the dose response curve for ^{60}Co γ-rays.

The RBE_M is the maximum value that can be assigned to the relative biological effectiveness of neutrons when the dose approaches a minimum. This was shown for the different donors as a function of the inherent radiosensitivity (α-values) to ^{60}Co γ-rays (Fig. 3.6). A statistical significant relationship (R^2= 0.8349, p = 0.0002) was noted between the reduction in neutron RBE_M values and an increase in the radiosensitivity of donor lymphocytes to ^{60}Co γ-rays.

Results from the present study were compared to that of a previous study for the same neutron beam (Fig. 3.6). MN formations in the study of Slabbert *et al*. (2010) were obtained using conventional microscopy. Also the ^{60}Co γ-ray doses used in their study ranged between 1 Gy to 5 Gy, the minimum doses used is thus much higher than that used in the current study. As a result the value of the initial slope for lymphocytes of each donor is better estimated using the semi-automated method.

RBE values from this study were for the most part compatible to that noted before. Vral *et al*. (1994) reported a mean RBE_M value for 5.5 MeV neutrons of 7.6 for lymphocytes obtained from 6 donors. A mean RBE_M value of 4.8 with a standard deviation of 4.2 was noted in the current study for a neutron source with a mean energy about six times higher. The lower RBE observed in the current study was consistent with the higher energy neutrons used. The mean RBE_M value of 5.3 reported by Slabbert *et al*. (2010) using the same neutron source, fall within the standard deviation of the results obtained. Mean RBE_M values of different studies were characterized by large standard deviations – as it should be when it is derived from cells obtained from different donors. As such the mean value was only of use to make simple comparisons with other studies. Even so one expected the general trend to change with neutron energy.

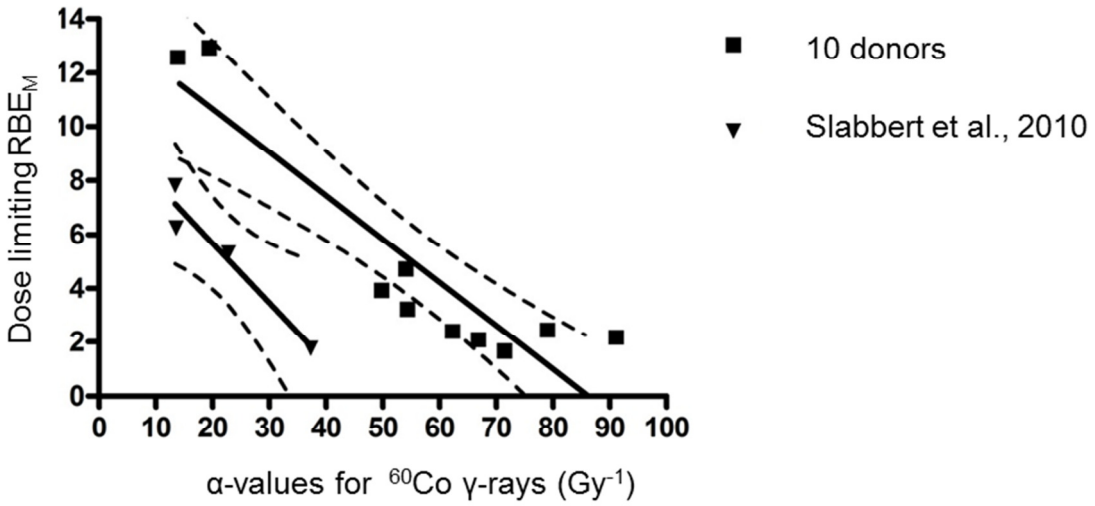

Figure 3.6: Dose limiting RBE_M values calculated for lymphocytes of different donors.

RBE As a Function of Neutron Dose

The dose response curves for the reference ^{60}Co irradiations were linear-quadratic in all cases compared to the more linear relationships between MN formations and neutron dose (Fig. 3.1). As a result systematic increase in neutron RBE could be expected at lower doses. The RBE values for neutron doses used in this study were calculated as follows:

$$RBE = \frac{\frac{\alpha}{2} + \frac{\sqrt{\alpha^2 + 4 \times MNF \times \beta}}{2}}{D_{\,neutrons}}$$

where the α and β are the dose response parameters that correspond to the MN formation frequency noted for a dose of neutrons ($D_{neutrons}$) applied in the study.

The formula employed is based on the solution of a quadratic equation. In this case the iso-effective ^{60}Co γ-rays dose ($D_{\gamma\text{-rays}}$) is calculated from the linear quadratic curve fit of the dose response curve for each individual. The isoeffect RBE is then calculated from the quotient of $D_{\gamma\text{-rays}}$ / $D_{neutrons}$ (Vandersickel *et al.*, 2010).

The relationship between neutron RBE and neutron dose is shown in Fig. 3.7 for all donors. In all cases an increase in neutron RBE was evident based on MN frequencies observed for lower neutron doses in comparison to the iso-effective dose of ^{60}Co γ-rays. The extent of the increase in RBE at lower doses was not the same for all donors. A maximum neutron RBE value at low doses of 10.8 was noted compared to a minimum of 3.4 amongst the cell samples used in the study.

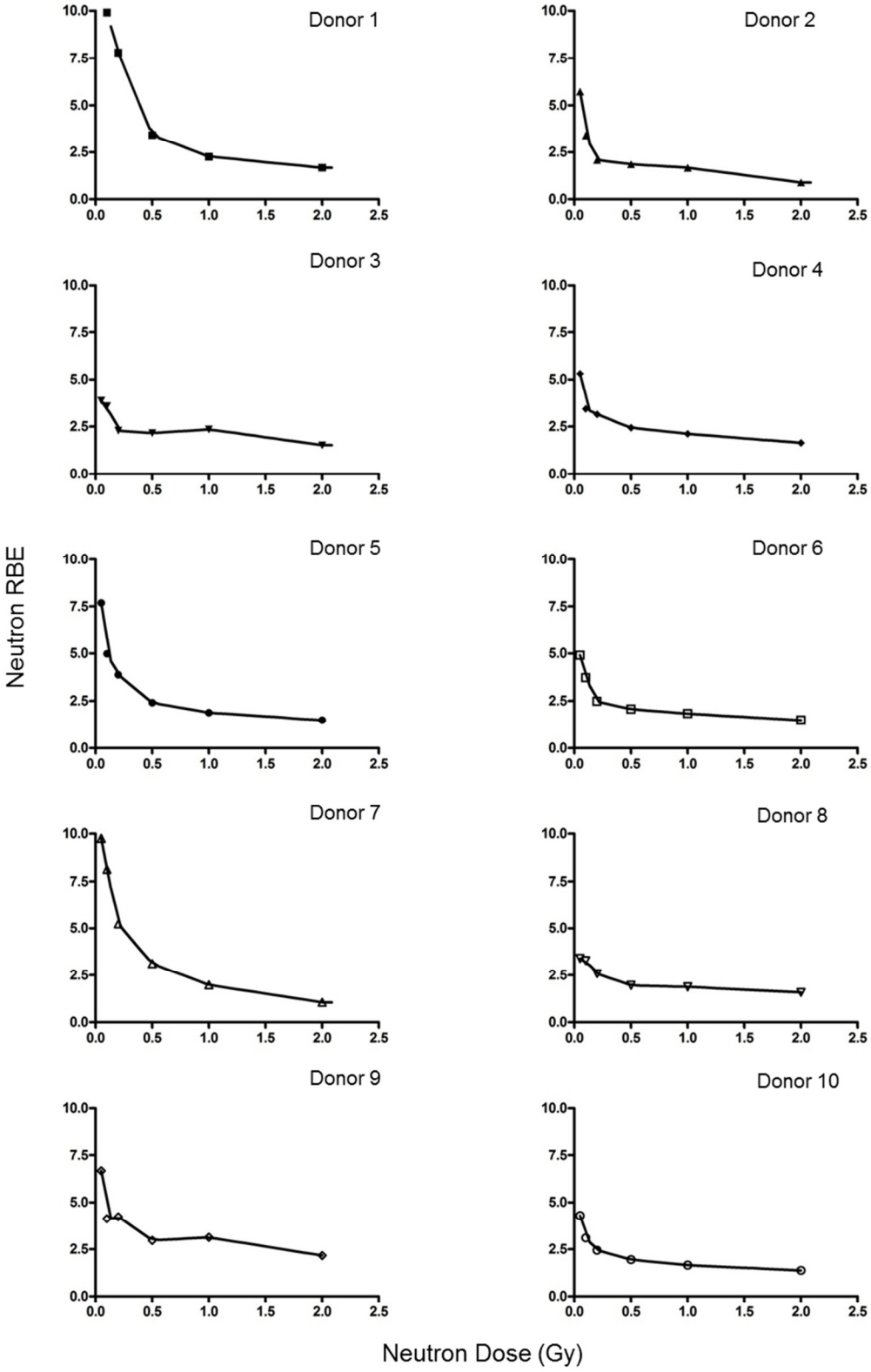

Figure 3.7: The relationship between neutron RBE values for different neutron doses applied in this study. An arbitrary line is fitted to the different values as a function of neutron dose and no underlying biophysical model is assumed.

It was of great interest to establish if the neutron RBE determined by this semi-automated image analysis system varied as a function of neutron dose compared with that expected from theoretical considerations (Kellerer and Rossi, 1978). The generalized formulation of the theory of dual radiation action is based in part on the observation that $\log_e$ (neutron RBE) as a function of $\log_e$ (neutron dose) is a straight line with a slope of -½ Gy^{-1} (Wambersie *et al.*, 1979). The mean neutron RBE values obtained in this study for all donors were plotted as a function of neutron dose (Fig. 3.8). The slope of the fitted line, -0.4 Gy^{-1} was consistent with similar relationships established for a wide variety of biological endpoints exposed to d(50)/Be neutrons (Wambersie *et al.*, 1979). Given the fact that RBE values can vary considerably between neutron doses of 0.1 Gy and 10 Gy, observed for chromosomal aberrations in plant cells to lung damage in mice, as quantified by these investigators, the slope of -0.4 Gy^{-1} determined for lymphocytes was compatible with these results.

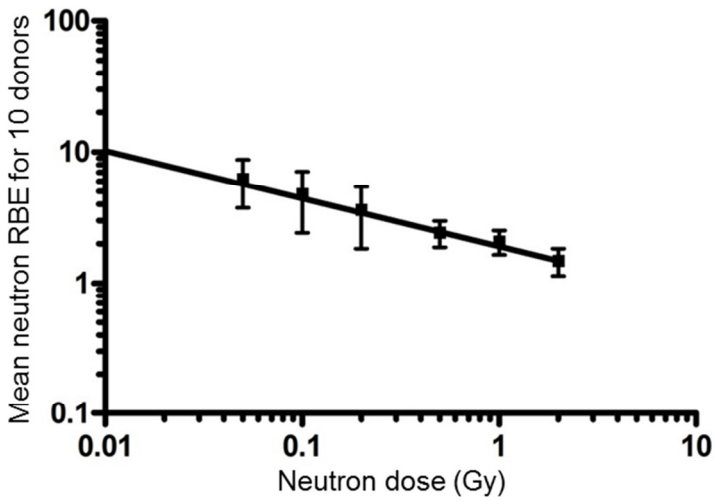

Figure 3.8: The mean neutron RBE values obtained in this study for all donors plotted as a function of neutron dose.

Chapter 4

Micronuclei Formations in Lymphocytes with Different Inherent Radiosensitivities to Auger Electrons Emitted By ^{123}I

Introduction

Differential variations in radiosensitivities of cells to low- and high-LET radiation are also important in nuclear medicine. In particular to understand targeted cell treatments employing radionuclides emitting low- and high-LET radiation using β- and α-emitters (Jansen *et al*., 2010 and Yong and Brechbiel, 2011). Several isotopes emitting Auger electrons are used in the treatment of disease (Morgenroth *et al*., 2011 and Terry and Vallis, 2012). These include: ^{55}Fe, ^{67}Ga, ^{99m}Tc, ^{111}In, ^{113m}In, ^{115m}In, ^{123}I, ^{125}I, ^{193m}Pt, ^{195m}Pt, ^{201}Tl, and ^{203}Pb (Chen, 2008). These particles have a distinct high-LET characteristic with RBE values around 12 which is comparable to that of alpha particles (Ginj *et al*. 2005). The identification of donors with lymphocytes with different inherent radiosensitivities noted in the previous chapter, allows one to investigate variations in response in relation to radioresistance using an Auger electron emitter.

However, to date no studies with human lymphocytes have been conducted where an Auger electron emitter has been incorporated selectively into the DNA of the cells. This is not surprising as the incorporation of a suitable organic compound labelled with an Auger electron emitter can only take place in cells that are actively dividing. Lymphocytes are in a permanent state of G_0 and will thus not normally integrate a nitrogenous base compound as part of the DNA.

Experiments are reported in this chapter that are aimed at establishing a protocol for the use of a radioactive halogenated pyrimidine to study Auger electron damage in lymphocytes.

Materials and Methods

Isotope Used in this Study

^{123}I is produced weekly at iThemba LABS for use by the nuclear medicine community in diagnostic imaging. As a result it is readily available in large quantities for radiobiological research and without any cost implications. It is produced by bombarding a NaI target with 66 MeV protons. This results is the formation of ^{123}Xe with a $T_{1/2}$ of 2.08 hours that decays into ^{123}I. As the ^{123}Xe parent nuclide decays the ^{123}I daughter nuclide fraction increases. Radioactive equilibrium is reached within 5.5 hours post target bombardment.

^{123}I is a suitable radionuclide for use in radiobiological studies when the need for a labeled organic compound exists. The chemistry of this halogen is well understood. The relative short $T_{1/2}$ of 13.2 hours makes it possible to deposit biologically detectable quantities of radiation energy over a short period of time. By contrast many studies on the effects of Auger electrons are conducted using ^{125}I. This has a relatively long $T_{1/2}$ of 60 days and as a result cells need to be exposed to the isotope for weeks to accumulate enough disintegrations that result in detectable levels of biological damage since the uptake into cellular DNA is limited. Using long lived isotopes requires cryo-freezing (-196 ˚C) of cell samples in a mixture containing dimethylsulfoxide (DMSO). The latter is a free radical scavenger with radio-protective properties. It is much better to expose cell samples to the radionuclide under normal physiological conditions. This has been done using ^{123}I (Kassis *et al*. 1990, Slabbert *et al*. 1999 and Smit *et al*. 2001).

^{123}I emits a γ-ray with energy 159 keV. This energy is ideal for imaging using a NaI scintillation crystal since the efficiency of the detector is high over this energy range. Furthermore the radioactive decay cascade of this isotope comprises on average of 11 Auger electrons per disintegration (Lobachevsky and Martin, 2005). Also the short range of Auger electrons in the absorbing medium results in multiple ionizations in close proximity to the DNA molecule for DNA incorporated ^{123}I. This makes it a suitable candidate for use in targeted radiotherapy.

Radiosynthesis of 5-[^{123}I]iodo-2′-deoxyuridine

Auger electrons emitted by ^{123}I have a range in the order of 5 to 20 nanometers in cells (Kassis *et al*., 1990 and Karamychev *et al*. 2000). Therefore it is essential to incorporate the radionuclide into cellular DNA to effect biological damage. Extracellular disintegrations are of limited biological consequence (Slabbert *et al*. 1999). A well-established method is to make use of a halogenated pyrimidine, for example the thymidine analog 5-[^{123}I]iodo-2′-deoxyuridine ([^{123}I]IUdR) (Baranowska-Kortylewicz *et al*., 1991 and Kassis *et al*., 1998).

For this study labeling of ^{123}I to the precursor 5-trimethylstannyl-2′-deoxyuridine (TMS-UdR) was done by a radiochemist at iThemba LABS. This resulted in the compound shown in Fig. 4.1. In short an ion exchange reaction method was followed by adding 0.1 M phosphate buffered saline (PBS) pH 7.4 (35 µℓ), [^{123}I]NaI solution (2-3 µℓ; 140 MBq), a solution of TMS-UdR(20 µg) in ethanol (2 µℓ), and a solution of chloramine-T trihydrate (50 µg) in water (2 µℓ). The constituents were mixed in a Vortex mixer for 10-15 min and then a solution of $Na_2S_2O_5$ (30 µg) in water (3 µl) was added. To isolate the pure product fraction, the mixture was injected into a high-pressure liquid chromatography (HPLC) column and the fraction was collected between 23.2 and 24.6 minutes.

The activity of the fraction was measured in a radioactivity counter (Isocal II-Radionuclide Assay Calibrator). The collected fraction of [^{123}I]IUdR was diluted with RPMI 1640 growth medium to a final activity of 60 µCi/mℓ.

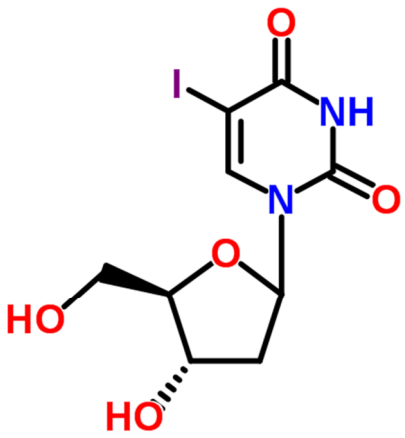

Figure 4.1: Chemical structure of of 5-[^{123}I]iodo-2′-deoxyuridine ([^{123}I]IUdR). Drawing from ChemSpider (CSID:10481938).

Incorporating [^{123}I]IUdR into Cellular DNA

[^{123}I]IUdR is built into the cell DNA during the DNA synthesis phase (S-phase) of the cell cycle. To ensure that [^{123}I]IUdR is incorporated as part of the DNA the cells in cultures used in the study must be dividing actively. Only then will cells in S-phase be available to take up the labeled compound. This needs to be verified before radiobiological investigations can be done. Also the purity of the preparation of the [^{123}I]IUdR needs to be tested as it can adversely affect the kinetics of cells in cultures.

Cell Culture Kinetics After Exposure to [^{123}I]IUdR

Cell kinetics in a long term presence of [^{123}I]IUdR, prepared as described above, was followed in Chinese hamster ovary cells (CHO-K1). These epithelial cells have a doubling time of about 12 hours and have more than 40 % of cells in S-phase at any one time (Theron *et al*., 1997 and Nakahara *et al*. 2002).

Exponentially growing CHO-K1 cells were trypsinized by adding 1 mℓ 0.05% trypsin to the growth flask after the medium was decanted aseptically. Cells were exposed briefly to trypsin before it was removed. The proteolytic action of the trypsin

hydrolyses protein thus releasing the cells from the surface of the culture flask. Cell cultures were incubated for 3 min where after they were resuspended in 10 mℓ RPMI 1640 growth medium. The FBS in the medium inactivates the proteolytic action of trypsin.

Cells were counted using a Neubauer hemocytometer. From the stock cell suspension multiple 2 mℓ cultures in 24 well plates were prepared. Then 100 000 cells were plated per well. The cultures were incubated for 4 hours to allow cells to attach to the growth surface. Then 50 µℓ [^{123}I]IUdR (6 µCi) was added to each well. For comparison 50 µℓ [^{123}I]NaI (6 µCi) was added to a different set of wells. As a control, cell cultures in some wells were left untreated.

Cell cultures were incubated for 24 hours at 37 ˚C and 5 % CO_2. Post incubation the medium was removed and the cell monolayers fixed with a 2 mℓ solution of buffered formalin. Using a phase contrast microscope (Nikon Model TMS) it was observed that the 100 000 cells seeded had initially multiplied but were still in a state of sub confluence. The fixative was removed after 10 minutes and a 1 mℓ 0.01 % crystal violet solution added to stain the cells. After 1 minute, the wells were rinsed in a basin using tap water and the plates were left to air dry. The stain absorbed in the monolayers of cells was released by adding 1 mℓ 10 % sodium lauryl sulphate (SDS) solution to each well. Plates were then incubated at 37 ˚C overnight. The optical density of the solution in each well was measured at 590 nm using a HP diode array spectrophotometer. The optical density represents a measure of cell growth in cultures treated with [^{123}I]IUdR. By comparing it to control cultures the underlying cell kinetics were revealed.

Cell Cycle Dependent Uptake of [^{123}I]IUdR

Peripheral blood T-lymphocytes do not normally divide and remain in the G_0 phase of the cell cycle. A different method of cell preparation from that described in Chapter 2, is needed to incorporate [^{123}I]IUdR into lymphocytes. For this isolated T-lymphocytes were stimulated with the mitogen PHA (Sigma-Aldrich), 44 hours before radiation treatments were done. Typically this started on a Monday and the time of

adding the PHA (Sigma-Aldrich) was judged to coincide with the availability of [^{123}I]IUdR the following Wednesday.

After 44 hours of culture time G_0 cells have progressed through the cell cycle to the S-phase allowing uptake of [^{123}I]IUdR. To 4 S-phase rich cultures [^{123}I]IUdR was added to final concentrations of 20, 40, 60 and 80 µCi/mℓ respectively. This was repeated for 4 un-stimulated, S-phase deficient cell cultures. The cultures were incubated for 2 hours to allow incorporation of the [^{123}I]IUdR into cellular DNA. Thereafter cell culture tubes were centrifuged at 180 g. for 5 minutes. The extracellular radioactivity was removed by aspirating the supernatant and adding 7 mℓ cold PBS. This PBS rinse step was repeated three times to remove residual extracellular radioactivity. Following centrifugation at 180 g. for 5 minutes, cell pellets were isolated by aspirating the PBS. Cell pellets were then lysed with 1 mℓ 1M NaOH and the contents of each tube was transferred to 5 mℓ glass test tubes to quantify the radioactivity.

The radioactivity of the contents of each tube was measured in a γ-counter (LB 2111 Berthold Multi Crystal gamma counter). The counts per minute (cpm) obtained from the γ-counter were converted to counts per second (cps) and then disintegrations per second (dps), assuming 91 % detector efficiency (E) and finally to activity as follows:

$$cps = cpm/60$$

$$dps = cps/E$$

$$A = dps/3.7 \times 10^{10}$$

Where A represents the Activity measured in curie (Ci).

Radioactive decay corrections were made to relate the measured activity to the activity (A_0) added to cell cultures at a reference time as follows:

$$A_O = \frac{A_T}{e^{-\lambda t}}$$

where $\lambda = \frac{\ln(2)}{T_{\frac{1}{2}}}$

A_T – Activity measured at time T

A_0 - Activity at reference time

λ - decay constant

t – time between measurement and experimental reference time

$T_{½}$- half-life

MN Response Observed in Lymphocytes Following Exposure to [^{123}I]IUdR

To investigate the biological response induced by Auger electrons incorporated into cellular DNA by [^{123}I]IUdR, S-phase rich lymphocyte cultures were exposed to different concentrations [^{123}I]IUdR. For this isolated T-lymphocytes were stimulated with the mitogen PHA (Sigma-Aldrich) 44 hours before radiation treatments were done.

After 44 hours of culture time G_0 cells have progressed through the cell cycle to the S-phase allowing uptake of [^{123}I]IUdR. To S-phase rich lymphocyte cultures [^{123}I]IUdR was added to final concentrations of 40 and 80 µCi/mℓ respectively. The cultures were incubated for 2 hours to allow incorporation of the [^{123}I]IUdR into cellular DNA. Pulse labeling was terminated after 2 hours by centrifugation at 180 g. for 5 minutes and aspirating the extracellular activity. Cells were rinsed 3 times with RPMI 1640 growth medium by centrifugation at 180 g. for 5 minutes and replacing the RPMI 1640 growth medium. Culture volumes were then reduced to 1mℓ by centrifugation at 180 g. for 5 minutes and removing the excess growth medium. Cultures were kept in a dark sterile biological safety cabinet at room temperature (18 ˚C) for 22 hours to allow the accumulation of disintegrations.

Culture volumes were then adjusted to 5 mℓ with RPMI 1640 growth medium warmed to 37 ℃. PHA (Sigma Aldrich) concentration of 20 µg/mℓ was maintained

and cytochalasin B (Sigma-Aldrich) which inhibits cytokinesis was added to a final concentration of 3 µg/mℓ. Cultures were incubated for another 24 hours at 37 ℃ and 5 % CO_2 to arrest cells in the binucleated state. After a total of 92 hours cultures were terminated, cells were fixed and microscope slides prepared and MN formations numerated as described in Chapter 2.

MN Response of Lymphocytes from Donors with Different Inherent Radiosensitivity Following Exposure to [^{123}I]IUdR

In chapter 3, inherent radiosensitivity differences in lymphocytes obtained from 10 donors was established after exposure to ^{60}Co γ-rays. Following exposure to high-LET radiation a decrease in differential radiosensitivity has been observed for different cell lines (Niemantsverdriet, 2012). To assess the biological effect of high-LET Auger electrons on the inherent radiosensitivity variations observed in lymphocytes obtained from different donors, lymphocytes from 3 donors identified as being radioresistant (donor 4), radiosensitive (donor 3) and of intermediate radiosensitivity (donor 8) were treated as follows:

Lymphocyte cultures obtained from the 3 donors were prepared in 10 mℓ tissue culture tubes. The lymphocytes in the cultures were stimulated to divide as described in the protocol above.

After 44 h incubation time, [^{123}I]IUdR , was added to the S-phase rich cultures to a final concentration of 45 µCi/mℓ. One culture per donor was not treated. Pulse labeling was terminated after 2 hours by removing the extracellular activity through repeatedly rinsing the cells with fresh RPMI. Culture volumes were reduced to 1 mℓ. Cultures were kept in a dark sterile biological safety cabinet for 22 hours to allow the accumulation of disintegrations.

Culture volumes were adjusted to 5 mℓ with complete RPMI medium warmed to 37 ℃. PHA (Sigma-Aldrich) was added to a final concentration of 20 µg/mℓ and cytochalasin B (Sigma-Aldrich) which inhibits cytokinesis was added to a final concentration of 3 µg/mℓ. Cultures were placed in the incubator for another 24 hours.

After a total of 92 hours cultures were terminated. Cells were fixed and microscope slides prepared as described in Chapter 2.

Results

Cell Culture Kinetics After Exposure to [^{123}I]IUdR and [^{123}I]NaI

In this study a compound was prepared that allowed ^{123}I to be incorporated into cellular DNA using the thymidine analogue [^{123}I]IUdR. Before this could be used for radiobiological studies, it was imperative to assess the effects of chemicals used in the synthesis of the compound on the kinetics of cell cultures in which it was used. A number of different methods to prepare [^{123}I]IUdR other than the method used in this study, failed to incorporate [^{123}I]IUdR into cellular DNA. This is thought to be due mainly to the cellular kinetics being adversely affected by chemicals used in the preparation. The testing of these compounds is not reported here as they showed little promise. In all cases a severe slowdown in cellular kinetics was evident using simple phase contrast microscopy. As a result there was no need for a quantitative analysis of cell growth.

The synthesis of [^{123}I]IUdR using the method reported here resulted in cells undergoing normal growth when exposed to the compound overnight. As a result a quantitative method using crystal violet stain was used to assess the suitability of the compound. The optical densities reflecting cell concentrations for treated and untreated cell cultures following a 24 hour exposure are shown in Fig. 4.2. No difference was noted in the growth rate of cell samples exposed to [^{123}I]IUdR or [^{123}I]NaI and control samples.

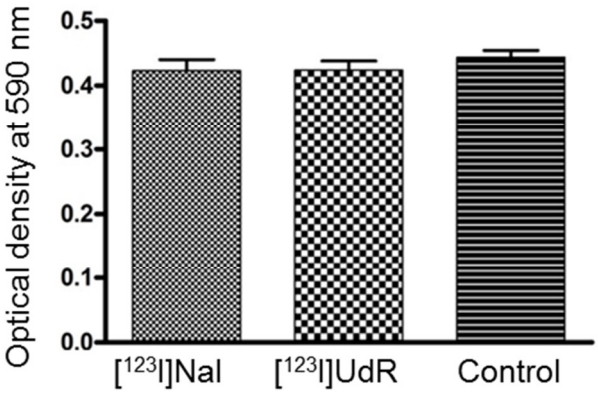

Figure 4.2: Optical densities of SDS solutions containing crystal violet reflecting the cell concentrations for treated and untreated cell cultures following an exposure period of 24 hour of cell cultures prepared in a multiwall plate and treated with the compounds indicated.

Radioactivity Uptake by Lymphocyte Cultures

Due to the complex culture method needed to incorporate [^{123}I]IUdR into S-phase lymphocytes it was essential to establish if the protocol described under Materials and Methods Chapter 2, resulted in successful uptake of [^{123}I]IUdR and if cells could be successfully cultured following a 22 hour period of standing at room temperature. All the cultures in this study proved to be successful in stimulating lymphocytes into S-phase and allowing uptake of [^{123}I]IUdR (Fig. 4.3).

The thymidine analogue [^{123}I]IUdR was selectively incorporated into cellular DNA for lymphocytes with an S-phase fraction. Higher radioactivity counts were seen in lymphocyte cultures stimulated with PHA compared to unstimulated lymphocytes. The radioactivity reading shown in Fig. 4.3 is that of lymphocyte culture samples that had been pulse labelled for 2 hours using different concentrations of [^{123}I]IUdR. Lymphocytes were washed 3 times with cold PBS and then the radioactivities were determined. The readings show an increase in the radioactive count with the amount of [^{123}I]IUdR added to the original cell cultures. Un-stimulated cells, by contrast show much lower levels of radioactivity. A small increase with an increase in activity added to the cultures is noted. This is likely to be as a result of the 3 PBS wash steps used not fully removing non-specific radioactivity.

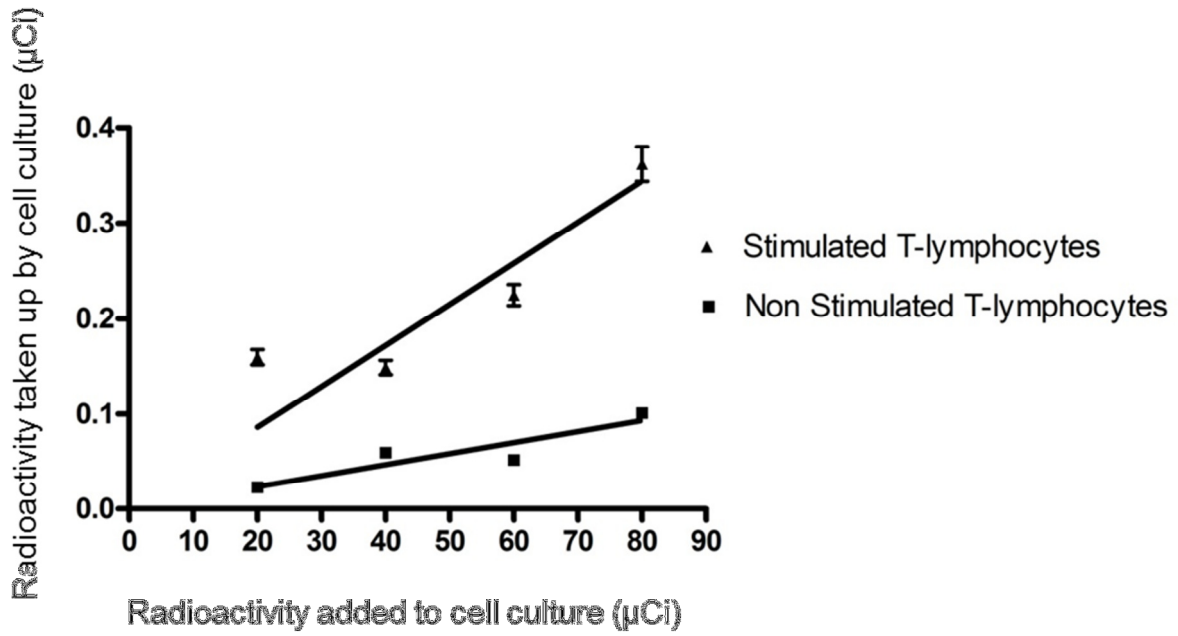

Figure 4.3: Comparison of [^{123}I]IUdR uptake for stimulated T-lymphocyte cultures (S-phase rich) and non-stimulated lymphocyte cultures (S-phase deficient).

MN Formation in Response to Auger Electron Damage

Following the pulse labelling of cells with [^{123}I]IUdR, unbound activity was removed by washing the cells 3 times with cold PBS. Then cell suspensions were left for 22 hours at room temperature in a laminar flow cabinet. Then cytochalasin B was added to the cell suspensions and then the lymphocytes were re-cultured at 37 ˚C for an additional 28 hours. It was important to establish if this complex culture process which is needed to incorporate the [^{123}I]IUdR and then allow accumulation of disintegrations, would successfully result in BN cells that can be analysed for MN formation. Therefore, the nucleation indices and percentage BN cells observed in the cell cultures of the 3 different donors are listed in Table 4.1. The percentage BN cells ranged between 34 and 44 %. This is consistent with the percentage BN cells observed in Chapter 3 following a less disruptive cell culture method. In these normal culture procedures the percentage BN cells for cultures ranged between 23 and 59 %. Moreover some cells in the experimental group contained 3 and 4 main nuclei which is an indication of cells dividing normally.

Table 4.1: Number of cells containing different numbers of main nuclei seen in cultures for 3 different donors. This reflects the cell culture kinetics of lymphocytes.

	1 Nucleus	2 Nuclei	3 Nuclei	4 Nuclei	Nucleation index	Percentage BN
Donor 3	60	39	1		1.44	39.39
Donor 4	53	42	5		1.52	44.21
Donor 8	64	34	1	1	1.35	34.69

MN Response Observed in Lymphocytes Following Exposure to [^{123}I]IUdR

The cytogenetic response of T-lymphocytes exposed to [^{123}I]IUdR was evaluated by enumerating MN frequencies in treated samples. MN frequencies induced by pulse labelling of cell cultures with 40 µCi/mℓ were more than that of the mean background of 8 MN per 500 BN cells. Cultures pulse labelled with 80 µCi/mℓ [^{123}I]IUdR resulted in MN formations more than double that seen for 40 µCi/mℓ (Fig. 4.4). The importance of this result is twofold. Firstly the abnormal culture conditions do result in the formation of increased measurable levels of MN. Secondly, the information obtained from these readings are indicative of how much activity should be used in pulse labelling.

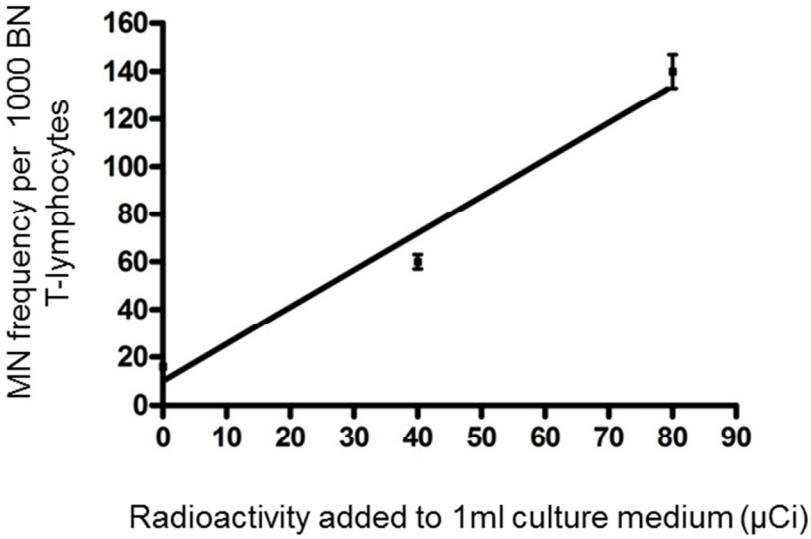

Figure 4.4: Micronuclei induction in T-lymphocytes following pulse labelling with different radioactivity concentrations.

MN Response of Lymphocytes from Donors with Different Inherent Radiosensitivity Following Exposure to [^{123}I]IUdR

MN formations induced in lymphocytes obtained from 3 donors with different inherent radiosensitivities were followed after pulse labelling with 45 µCi/mℓ [^{123}I]IUdR. The two hour pulse labelling of stimulated lymphocytes with 45 µCi/mℓ resulted in 0.2 µCi being incorporated into the DNA of the stimulated lymphocyte fraction. This reading represents the mean radioactivity for lymphocyte cultures from 3 different donors after cells were repeatedly washed with PBS. The decay of 0.2 µCi over a period of 22 hours resulted in the irradiation of cellular DNA with Auger electrons from ^{123}I. This treatment induced 53, 56 and 58 MN per 1000 BN cells respectively amongst the 3 donors used in the study (Fig. 4.5). This is slightly lower than the results obtained in the dose finding experiment (Fig. 4.4).

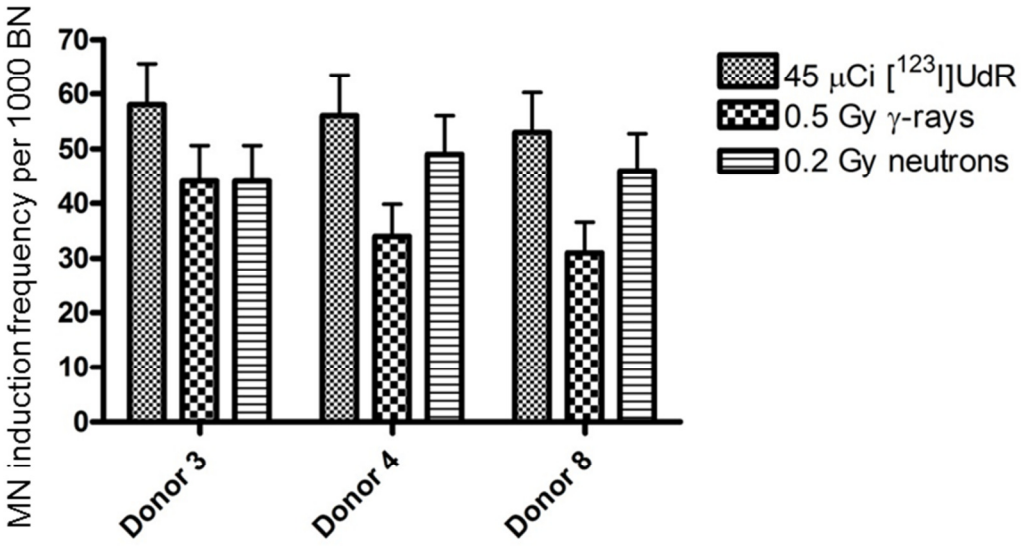

Figure 4.5: Biological dose response variations for 3 donors with predetermined inherent radiosensitivity differences exposed to different radiation qualities. Donor 3 was found to be most radiosensitive and donor 4 most radioresistant to ^{60}Co γ-rays.

The variation in MN formations induced in lymphocytes obtained for donors with different inherent radiosensitivities following pulse labelling with 45 μCi/mℓ [^{123}I]IUdR needs to be compared with that for MN formations in lymphocytes obtained from the same donors exposed to ^{60}Co γ-rays and neutrons. For this MN formations for each donor noted after doses of ^{60}Co γ-rays or neutrons that are closest to that seen for Auger electrons are compared. The coefficient of variation (CV) of MN induction by Auger electrons for the three donors is 4.5 % (Table 4.2). This compares to a CV of 5.4 % for exposure to neutrons and a CV of 18.7 % for ^{60}Co γ-rays. A larger than threefold increase in the variations in response of different donors to high-LET radiation modalities are noted compared to ^{60}Co γ-rays (Table 4.2). This is notwithstanding the fact that higher levels of biological damage for neutrons and Auger electrons are compared to that for γ-rays. Moreover the variation in responses to Auger electrons of lymphocytes from different donors with established differences in inherent radiosensitivities is marginally less than that of neutrons. A systematic reduction in the coefficient of variation in response is thus noted with an increase in the ionization density used in the treatment of T-lymphocytes (Fig. 4.5).

Table 4.2: The coefficient of variation (CV) for MN formations in lymphocytes from 3 donors with an established difference in inherent radiosensitivities.

Radiation modality	Mean number MN per 1000 BN	Standard Deviation	Standard Error	Coefficient of variation
0.5 Gy ^{60}Co γ-rays	36.33	6.80	3.93	18.73%
0.2 Gy p(66)/Be neutrons	46.33	2.52	1.45	5.43%
45 µCi [^{123}I]IUdR	55.67	2.52	1.45	4.52%

Biological Effectiveness by Auger Electrons Induced by [^{123}I]IUdR Compared to that Induced by [^{123}I]antipyrine and [^{123}I]NaI

The only other study available in the literature where the effects of Auger electrons were followed in T-lymphocytes was that by Slabbert *et al*. (1999). Using ^{123}I labelled to the organic compound antipyrine. Antipyrine allows ^{123}I to cross the cell and nuclear membrane. MN formations were observed and compared to that noted in CHO-K1 cells. As a control irradiation, lymphocytes and CHO cells were exposed to [^{123}I]NaI that is not taken up by cells, however cells are exposed to the 159 keV γ-ray emitted by ^{123}I. Large variations in the response of lymphocytes (radioresistant cells) and CHO cells (radiosensitive cells) are noted for exposure to [^{123}I]NaI. A much smaller variation in the response of these cell types is noted when exposed to [^{123}I]antipyrine where the Auger electrons emitted by ^{123}I effect cellular damage. The data obtained for [^{123}I]IUdR is consistent with this.

To compare the differences in efficiency of inducing MN formations by [^{123}I]IUdR with that by [^{123}I]antipyrine, the number of disintegrations per unit volume for the

radioactivity incorporated into the cellular DNA of lymphocytes used in this study needs to be calculated. The number of nuclear disintegrations per 1 mℓ culture volume was calculated for the radioactivity incorporated into cells and allowed to decay for 22 hours. The total number of disintegrations divided by the volume of the culture is expressed disintegrations per cubic micrometre ($d/\mu m^3$).

The mean MNF induced by [^{123}I]IUdR in the lymphocytes of 3 donors was 56 MN per 1000BN. The number of disintegrations per micrometre needed to yield this frequency is 4 $X10^{-4}$ $d/\mu m^3$. This compares to 8 $X10^{-2}$ $d/\mu m^3$ for lymphocytes treated with [^{123}I]antipyrine.

Chapter 5

Discussion

In this study the accuracy of a semi-automated image analysis system to detect differences in inherent radiosensitivities of lymphocytes obtained from different donors exposed to different radiation qualities was assessed. This was done to determine radiation weighting factors for a high energy neutron beam.

Micronuclei induction in lymphocytes was chosen as the biological endpoint to measure RBE differences of high energy neutrons with respect to ^{60}Co γ-rays the reference radiation. Cytogenetic damage in lymphocytes has been well documented by several authors for such studies (Huber *et al*., 1992, Mill *et al*., 1996, Schmid *et al*., 2002 and Slabbert *et al*., 2010). Furthermore MN induction has been shown to be a suitable endpoint to quantify lymphocyte radiation damage using a semi-automated image analysis system (Verhagen and Vral, 1994 and Vral *et al*., 1994).

Cell Cultures

MN formations following radiation damage can only be observed if T-lymphocytes samples have been successfully stimulated to complete nuclear division (IAEA, 2011). MN frequencies were therefore numerated only in BN cells, as this is a verification that cells have completed nuclear division. The cell culture methods employed in this study proved to be most suitable as only one failure had been noted out of 144 cultures set up for this study. The nucleation indices observed representing the mitogenic response of the cells in culture were much larger than 1 (Table 3.1). This is an indication that a significant fraction of lymphocytes completed at least one nuclear division. The lowest percentage BN in a culture was 23 %. This represents 230 000 BN cells available for analysis compared to about 2000 BN cells needed to quantify MN.

Dose Response Curves

Background Readings

A notable disadvantage of the MN assay is the variable spontaneous background MN frequencies between different donors. Spontaneous variation in background MNF ranging from 0 to 40 MN per 1000 BN cells have been reported in human lymphocytes (Verhagen and Vral, 1994, Vral *et al*., 1994, Wuttke, 1998 and Fenech, 1999). Several studies have shown that apart from exposure to clastogens, the biggest contributing factors to spontaneous MN are age and gender (Fenech *et al*., 1999). Background readings noted in this study ranged from 4 to 15 MN per 1000 BN cells and thus is not as variable as that noted by other investigators. A possible explanation for this is that only health donors within a working age were used in this study. The variable spontaneous background in MNF limits the sensitivity of detection of damage induced by low doses of radiation (Mill *et al*., 1996). The mean spontaneous MN frequency for male donors was 7 ± 0.8 whilst that for females was 12 ± 2.1. The higher spontaneous MNF noted for female donors was consistent with that noted in previous studies (Thierens *et al*. 2000 and Pala *et al*, 2008).

Radiation Induced MN

The detection limit of radiation induced MN is reported to be 0.2 to 0.3 Gy (Vral *et al*., 2011). In this study an increase in MNF above the background was noted for 6 donors for a dose of 0.05 Gy ^{60}Co γ-rays. The increase in MNF was however not statistically significant when comparing the data for all donors used in the study. For a dose of 0.1 Gy, ^{60}Co γ-rays, 7 donors displayed MNF significantly higher than background readings. The other 3 donors only display significant differences for doses higher than 0.2 Gy. It is concluded that the image analysis system is able to detect readings from the background for 70 % samples at 0.1 Gy and 100 % samples at 0.2 Gy. The higher precision of the Metafer system is likely the result of consistent readings using the same image analysis classifier.

The ability to detect differences in MNF after lower doses in this study will have contributed to the accuracy in construction of dose response curves for lymphocytes obtained from each donor in the study. Higher α-values for ^{60}Co γ-rays were noted compared to those of previous studies (Vral *et al*., 1994 and Slabbert *et al*., 2010). Close inspection of the aforementioned studies reveal that MN formations were not quantified over the same low dose range used in the current study. Using low dose points of 0.05, 0.1 and 0.2 Gy ensures an accurate estimate of the initial slope of the dose response curve represented by α-value (Malaise *et al*., 1994 and Ono, *et al*. 1994).

Dose response curves determined using the automated scoring system for both high- and low-LET radiations exhibit distinct characteristics consistent with those noted using manually scoring methods in assessing radiation damage in lymphocytes (Slabbert *et al*. 2010) and in the estimation of cell survival (Hall and Giaccia, 2005). The MN response observed for each donor is higher after all doses of neutrons used in the study compared to the corresponding doses of γ-rays. This confirms the dependence of MN induction frequency as a function of radiation quality (Wuttke *et al*., 1998). Secondly, a clear linear-quadratic relationship is noted for γ-rays with β-values significantly larger than zero (Table 3.2). Typically DNA DSBs are induced by low-LET radiation as a result of 2 DNA lesions that are formed by two separate tracks of ionizing radiation. At low doses the probability of a coincidence of two DNA lesions in close proximity is small. At higher doses there is an increased probability of a coincidence of two single strand breaks in close proximity. In this dose region the biological effect is proportional to the square of the dose.

By contrast the overwhelming linear response noted for neutrons is in part due to the quality of the radiation of which the biological effect is proportional to the dose (Hall and Giaccia, 2005). In three of the 10 donors a significant β component was observed for the neutron irradiations. The bending component observed for these donors is due the ability of the affected cells to accumulate repairable damage. Furthermore the physical properties of p(66)/Be neutron beam used in this study are such that about 36% of the dose is induced by secondary charged particles that overlaps with the ^{60}Co γ-ray spectrum (Slabbert *et al*., 1989).

95 % Confidence Ellipses

Distinct differences in dose response curves for the different donors to ^{60}Co γ-rays were observed. To qualify inherent radiosensitivity differences at the 95 % confidence level, ellipses have been constructed that relate the covariance parameters of α and β that determine the dose response curve for lymphocytes from each donor. The mean and variances were used to calculate a set of α and β coordinates that demarcates the 95 % confidence interval (Sokal *et al*., 1995). Thus the ellipse represents the inherent radiosensitivity of an individual (α-value) as well as the capacity to accumulate repairable damage (β-value). The confidence ellipses around the mean α- and β-value estimated were separate for most donors. The only exceptions were those for donors 5 and 7 and 5 and 8 (Fig. 3.2). To identify different inherent radiosensitivities in lymphocytes of different donors it is important that the confidence ellipses for dose curves must be relatively small. The automated image analysis results in consistent MNF counts that follow the fitted dose response curves very closely. The consistent MN detection of the Metafer is most likely the principal reason why lymphocytes form 8 of the 10 donors proved to have statistically significant variations in their radiosensitivities to ^{60}Co γ-rays. The α-values observed in the study ranged from 13 to 91 Gy^{-1} and thus vary by a factor of 7.

Confidence ellipses noted for neutron irradiations are relatively larger for all donors and also cluster together with several overlapping (Fig. 3.3). The relative larger 95 % confidence ellipses noted for neutron irradiations is the result of using fewer dose points over a smaller dose range compared to that used for ^{60}Co γ-rays. Survival curves for different types of clonogenic mammalian cells exposed to 300 kV X-rays or 15 MeV neutrons, showed markedly less variation in radiosensitivity for cells irradiated with the neutrons (Hall and Giaccia, 2005). The smaller variation in radiosensitivity exhibited by these cells is characteristic of the local dose deposition nature for this type of radiation, thus a lack of sublethal repair is apparent (Barendsen, 1994).

Using the ellipses in Fig. 3.2 donors were ranked according to their radiosensitivity to low-LET ^{60}Co γ-rays and this is compared to the ranking of individuals' lymphocytes to neutrons (Fig. 3.3). The donors radiosensitivity rank established for ^{60}Co γ-rays

did not follow the same trend after exposure to p(66)/Be neutrons (Fig. 3.4). This demonstrates a reduced variation in the relative radiosensitivity of lymphocytes from different donors to γ-rays and neutrons. A similar observation was published for mammalian cell lines exposed to ^{60}Co γ-rays and a 15 MeV neutron beam (Broerse and Barendsen, 1973).

Dispersion Parameters

The dispersion indices for MN formations noted in lymphocytes is an indication whether the automated image analysis system used in the study is able to detected qualitative differences in radiation quality. Comparing $\sigma^2/\bar{y}$ for ^{60}Co γ-rays and p(66)/Be neutrons, showed that MN formations in lymphocytes were consistently more over-dispersed for neutron irradiations compared to ^{60}Co γ-rays (Fig. 3.5).

Statistically significant ($\mu > 1.96$) over-dispersed distributions were noted in the number of MN observed in cells following exposure to ^{60}Co γ-rays or neutrons. However the mean μ-value of 3.92 for cell samples exposed to ^{60}Co γ-rays was significantly less than the corresponding μ-value of 7.05 for neutrons. This implies that the spatial distribution of ionization events induced by neutrons is readily detectable using the automated image analysis system.

Relative Biological Effectiveness

RBE is a complex quantity dependant on several factors including radiation quality, radiation dose, fractionation protocol, dose rate and the biological system or end point used in its estimation (Hall and Giaccia, 2005). Biological end points such as clonogenic cell survival (Thomas *et al*., 2007), jejunal crypt regeneration (Gueulette *et al*., 2005), dicentric formations in lymphocytes (Nolte *et al*., 2007) and MN induction in lymphocytes (Slabbert *et al*., 2010) have been used with great success to determine RBE of different radiation qualities. Using apoptosis in lymphocytes as an endpoint to determine RBE for a 280 keV neutron beam compared to ^{137}Cs γ-rays, Ryan *et al*., (2006) found the RBE to be close to one. By contrast Nolte *et al*., (2007) noted an RBE of approximately 90 for the same energy neutron beam, but

using dicentric formations in lymphocytes as endpoint. The latter is however a very time consuming method. The quantification of apoptosis in cells with a flow cytometer is a well described process enabling the user to analyse large numbers of cell samples over a short period of time (Lacombe and Belloc, 1996 and Darzynkiewicz *et al*., 2001). But this endpoint is not able to discern between different radiation qualities and yield RBE values larger than 1. It is thus important to choose an appropriate endpoint for doing such studies. Micronuclei formations in lymphocytes proved to be a suitable endpoint to determine radiation damage on a cytogenetic level. In the past cytogenetic damage expressed as MN has been used to distinguish between radiation damage induced by different radiation modalities with success (Vral et al., 1994 and Slabbert et al. 2010). When radiation weighting factors are assigned to different radiations, the probability of inducing neoplastic disease is investigated. Hence cytogenetic damage has to be related to the radiation quality. Furthermore MN enumeration is now possible using semi-automated image analysis (Willems *et al*. 2009). It is thus appropriate to study this endpoint using the Metafer microscope system.

The principal objective of this study was to establish if high energy neutron RBE_M values and a variation in the inherent radiosensitivity of lymphocytes from different donors to ^{60}Co γ-rays are related. The range and variation of inherent radiosensitivity represented by the α-values for ^{60}Co γ-rays (Fig. 3.6) are marginally higher than that reported previously (Slabbert *et al*. 2010). To date there is no other data available for high energy neutrons to compare with the current study.

A clear correlation between neutron RBE_M values and radiosensitivity of donor lymphocytes to ^{60}Co γ-rays could be established. This finding using 10 donors confirm the conclusions made by Slabbert *et al*. (2010) using the results of 4 donors exposed to the same neutron beam. The RBE_M values noted in this study ranged from two to thirteen. The highest RBE_M values are those for the two most radioresistant donors. Values for the other 8 donors are consistent with that reported for this neutron beam (Slabbert *et al*. 2010). The greater variation in RBE_M values seen may be attributed in selecting in this study donors with bigger variation in inherent radiosensitivity differences to ^{60}Co γ-rays in this study. This is consistent with using a larger cohort of donors.

The mean neutron RBE_M determined for the 29 MeV neutron beam in this study is 4.8. This is lower than the mean RBE_M of 7.6 noted for a 5.5 MeV neutron beam (Vral *et al*., 1994). It is also lower than the RBE of 12.2 for micronuclei in lymphocytes exposed to a mixed fission neutron-gamma-ray beam reported by Hubber *et al*. (1994). The RBE of neutron beams is expected to increase with a decrease in neutron energy.

The mean RBE_M value of 4.8 determined in this study is consistent with mean RBE_M value of 4.2 reported previously for the same neutron source (Slabbert *et al*., 2010). Both these findings support the value of 9 found by Nolte *et al*., (2007) using dicentric formations in lymphocytes exposed to a 192 MeV beam. The RBE_M value of 113 for simulated neutron spectra at flight altitudes reported by Heimers, (1999) is clearly at variance with the results of the current study.

RBE_M values can be expected to remain unchanged for neutron energies above 20 MeV (Nolte *et al*., 2005).

The range of RBE_M values for a p(66)/Be neutron beam reported here is 3.5 to 12. Moreover the unequivocal relationship established in this study between neutron RBE and radioresistance points to the need to determine radiation weighting factors using cells from multiple donors. The study of Nolte *et al*., (2007) is thus incomplete and RBE_M values as a function of neutron energy needs to be established for both sensitive and radioresistant donors. The relationship between neutron RBE and radioresistance obtained in this study using a mean neutron energy of 29 MeV clarifies the need to obtain weighting factors at high neutron energies (>20 MeV). Moreover at energies lower than 20 MeV a correlation between neutron RBE and radioresistance can be expected. This has been demonstrated by Vral *et al*., (1994) for 5.5 MeV neutrons source and Slabbert *et al*., (2000) for a 6 MeV neutron source.

RBE as a Function of Neutron Dose

Mean neutron RBE values of all donors as function of dose are plotted in Fig. 3.8. The log neutron RBE_M is expected to relate to the log neutron dose as a straight line considering theoretical arguments by Kellerer and Rossi, (1978). The generalized formulation of the theory of dual radiation action is based in part on the observation that $\log_e$ (neutron RBE) as a function of $\log_e$ (neutron dose) is a straight line with a slope of -½ Gy^{-1}. In this study a slope of -0.4 Gy^{-1} is determined for lymphocytes. This is consistent with similar relationships established for a wide variety of biological endpoints exposed to d(50)/Be neutrons (Wambersie *et al.*, 1979). RBE values obtained by these investigators for diverse endpoints including chromosomal aberrations in plant cells to lung damage in mice spanning doses of 0.1 to 10 Gy approximate this theoretical slope of -½ Gy^{-1}. Given the variation in neutron RBE values for different cell types at different doses the slope of -0.4 Gy^{-1} noted in the current study for lymphocytes is in line with theoretical expectations.

Micronuclei Formations in Lymphocytes with Different Inherent Radiosensitivities to Auger Electrons Emitted By ^{123}I

In this part of the study micronuclei induction in lymphocytes was monitored to measure differences in cytogenetic damage induced by Auger electrons emitted by ^{123}I. This was done for ^{123}I incorporated into cellular DNA. This investigation is unique as a survey of the literature reveals that cytogenetic damage in lymphocytes has not been studied to date using a radioactive halogenated pyrimidine. It has been attempted as knowledge of cellular response in relation to radiosensitivity is also important in nuclear medicine applications using radionuclides emitting high-LET radiation.

The protocol followed in the chemical preparation of [^{123}I]IUdR proved to be suitable for studies using cells in culture. This was demonstrated by following the cell culture kinetics of CHO cells exposed to [^{123}I]IUdR and [^{123}I]NaI and compare it to that of untreated cell samples. The preparation method of [^{123}I]IUdR used in this study

demonstrated not to involve any chemicals that interfere with cellular kinetics. This allowed the incorporation of [^{123}I]IUdR into lymphocyte DNA.

The thymidine analogue [^{125}I]UdR is readily incorporated in cellular DNA replacing the pyrimidine nucleobase thymine during DNA synthesis (Sokolov *et al*., 2007). As such only cells in S-phase incorporate [^{123}I]IUdR into cellular DNA (Bradley *et al*., 1975). Peripheral blood lymphocytes normally reside in the G_0 phase of the cell cycle. Incorporation of [^{123}I]IUdR into cellular DNA during this phase of the cell cycle is not possible. Differential uptake of [^{123}I]IUdR between S-phase rich and S-phase deficient lymphocyte populations could clearly be demonstrated (Fig. 4.3). This confirms that cells were successfully stimulated and that detectable quantities of [^{123}I]IUdR could be incorporated into lymphocytes. To ensure effective uptake and incorporation of a radiolabelled compound the addition of [^{123}I]IUdR to cell cultures has to coincide with the period where most cells are actively synthesizing DNA (Vaidyanathan *et al*., 1996). It has been shown that the largest fraction of PHA stimulated lymphocytes enter a period of DNA synthesis between 48 and 72 h after stimulation (Sören, 1973). However cell cycle analysis of PHA stimulated lymphocytes reveals that only 10 to 20 % cells are in S-phase at any one time during this period (Darzynkiewicz *et al*., 1976). Cells were exposed to [^{123}I]IUdR starting at 44 hours and ending 46 hours post stimulation. Ideally the exposure period should be such as to expose all cells to [^{123}I]IUdR. However due to the short half-life of ^{123}I (13.2 hours) this is not practical as a substantial amount of radioactive decay over this period would lead to the incorporation of non-radioactive IUdR.

The prolonged cell culture method of 92 hours attempted in this study proved to be successful to allow the incorporation of [^{123}I]IUdR into lymphocytes and to effect the accumulation of enough disintegrations of the isotope to yield measurable cellular damage. From the lymphocytes of all three donors used in this study sufficient numbers of BN cells were obtained for microscopic analysis notwithstanding the fact that cell cultures were interrupted for 22 hours in the process. During this time lymphocytes were left at room temperature to allow decay of ^{123}I. This method can be used to study Auger electron damage from other isotopes in lymphocytes.

MN formations induced in lymphocytes obtained from 3 donors with established differences in inherent radiosensitivities were followed after pulse labelling with [^{123}I]IUdR. These three donors include a donor sensitive to γ-rays, resistant to γ-rays and a donor with an intermediate sensitivity to γ-rays. It is of interest to compare the variation in lymphocyte response to Auger electrons to that of ^{60}Co γ-rays and p(66)/Be neutron exposures. To achieve this MN in lymphocytes for the same three donors exposed to neutron and γ-rays are used for comparison (Fig. 4.5). MN formations to doses of neutrons and γ-rays closest to that seen for [^{123}I]IUdR treatments arre compared. Clear differences in the variation of biological response for the three different donors to the different radiation qualities are evident. Large dose response variations of up to 19 % are seen for ^{60}Co γ-ray exposures. This dropped to 5 % for neutrons and 4 % for Auger electron damage. This reduced variation in the lymphocyte response between donors sensitive and resistant to ^{60}Co γ-rays is consistent with the progressive increase in ionization densities of the treatment modalities. The differences in MN formations for lymphocytes from the three donors for neutron treatments relative to that for Auger electrons is less than expected. This is logical as Auger electrons are expected to have ionization densities similar to that of α-particles (Laster *et al*., 1996).

Considering that only about 10 to 20 % of lymphocytes are in S-phase during the pulse labelling period between 44 and 46 hours (Darzynkiewicz *et al*., 1976) only a limited fraction of the cells exposed to [^{123}I]IUdR in this study could be expected to incorporate the compound. A substantial number of cells will not incorporate [^{123}I]IUdR, hence not exhibit any cytogenetic damage. As a result the results reported here is most likely an underestimation of the biological damage by [^{123}I]IUdR.

The high-LET characteristics of Auger electrons have also been noted in other studies. Survival curves established for Auger electrons incorporated into DNA exhibit no shoulder at low doses (Makrigiorgos *et al*., 1990). Thus the β-component of the linear quadratic model that describes the cells' capacity to repair sublethal damage has disappeared. This finding is consistent with cells exposed to high-LET α-particle sources (Goddu *et al*., 1994).

Calculation of RBE values for DNA incorporated Auger electrons will be challenging as the dose deposition is confined to nanometre volumes. This can in principle be done using Monte Carlo simulations, but falls outside the scope of this investigation. In order to calculate an RBE for Auger electrons, lymphocyte samples will need to be exposed to different activities of ^{123}[I]IUdR that result in different levels of disintegrations in cellular DNA. The corresponding MN dose response curve can then be used in conjunction with the ^{60}Co dose response curve to estimate the RBE of Auger electrons.

Being able to incorporate [^{123}I]IUdR into lymphocytes it is now possible to compare the effect of Auger electrons delivered in this manner with that done using the same cell type as in previous studies with [^{123}I]antipyrine (Slabbert *et al*., 1999). Using the MN formations observed in three donors the number of disintegrations per cubic micrometre needed to induce 1 MN is calculated to be 7 x10^{-6} d/μm^3. This compares to 1 x10^{-3} d/μm^3 for lymphocytes treated with [^{123}I]antipyrine. Disintegrations by ^{123}I effected in cells when labelled to deoxyuridine is thus more than three orders of magnitude more efficient in inducing MN formations. This is logical as all the Auger electrons emitted by [^{123}I]IUdR are in close proximity to the DNA, whilst that of [^{123}I]antipyrine are not necessary within range of this critical target. From this it is clear that the therapeutic use of Auger electron emitters when labelled to an antibody or an organic compound that allows intra cellular disintegrations is highly efficient to induce cellular radiation damage.

The reduced variation in MN formations by Auger electrons for cells with different inherent radiosensitivities noted in this study has implications for selecting a suitable radionuclide for therapeutic purposes. In all probability the response of cancer cells with different radiosensitivities will vary when treated with a β-emitter. Treatment with an α-particle or Auger electron emitter is likely to result in a more uniform response. As a result it is reasonable to expect that the relative biological effectiveness of α-particle or Auger electron emitters will increase when used in the treatment of radioresistant disease (Barendsen, 1996). An increase in the RBE of Auger electrons with radioresistance can be inferred from these findings and constitutes a basis for therapeutic gain in treating cells compared to using radioisotopes emitting low-LET radiation (Todd, 1977). Consequently the response of cancer cell types with

established differences in inherent radiosensitivities should be followed to verify the therapeutic gain for its application in target radiotherapy.

Conclusions

1. The semi-automated image analysis system used in this study detects MN formations in peripheral blood lymphocytes accurately to show differences in the inherent radiosensitivity of different donors.

2. Quantitative and qualitative differences in MN formations in response to changes in radiation quality can be detected using the Metafer microscope system.

3. The MN assay is a suitable biological endpoint when investigating inherent radiosensitivity differences and related RBE values.

4. A clear relationship between neutron RBE and inherent radiosensitivity to ^{60}Co γ-rays could be established for high energy neutrons.

5. When determining radiation weighting factors for neutrons of all energies it is essential to base this on the cellular response of different donors.

6. Biological damage induced by Auger electrons can be studied in peripheral blood lymphocytes using the thymidine analogue [^{123}I]IUdR.

7. The high-LET characteristics of Auger electrons result in a reduced variation in the response of lymphocytes obtained from donors with different inherent radiosensitivities.

Reference List

Baranowska-Kortylewicz J, Makrigiorgos GM, Van den Abbeele AD, Berman RM, Adelstein SJ, Kassis AI. 5-[^{123}I]iodo-2'-deoxyuridine in the radiotherapy of an early ascites tumor model. Int J Radiat Oncol Biol Phys. 1991;21(6):1541-51.

Barendsen GW. Responses of cultured cells, tumors and normal tissues to radiation of different linear energy transfer. Curr Top Radiat Res. 1968;4:293-356.

Barendsen GW. The Relationships between RBE and LET for Different Types of Lethal Damage in Mammalian Cells: Biophysical and Molecular Mechanisms. Radiation Research. 1994;139:257-270.

Barendsen GW. RBE-LET relationships for lethal, potentially lethal and sublethal damage in mammalian cells: implications for fast neutron radiotherapy. Bull Cancer Radiother. 1996;83 Suppl:15s-8s.

Bradley EW, Chan PC, Adelstein SJ. The Radiotoxicity of Iodine-125 in Mammalian Cells: Effects on the Survival Curve of Radioiodine Incorporated into DNA. Radiation Research. 1975 Dec;64(3):555-563.

Broerse JJ, Barendsen GW. Relative biological effectiveness of fast neutrons for effects on normal tissues. Curr. Top Radiat Res 1973;8:305-350.

Burdak-Rothkamm S, Prise KM. New molecular targets in radiotherapy: DNA damage signalling and repair in targeted and non-targeted cells. Eur J Pharmacol. 2009;625(1-3):151–155.

Cardoso RS, Takahashi-Hyodo S, Peitl P, Ghilardi-Neto T, Sakamoto-Hojo ET. Evaluation of chromosomal aberrations, micronuclei, and sister chromatid exchanges in hospital workers chronically exposed to ionizing radiation. Teratog Carcinog Mutagen. 2001;21:431–439.

Cember H. Introduction to Health Physics. 1st ed. Oxford: Pergamon Press; 1969.

Cerruti M. Surface characterization of silicate bioceramics. Phil. Trans. R. Soc. 2012; 370:1281-1312

Chen J. A compilation of microdosimetry for uniformly distributed Auger emitters used in medicine. Int J Radiat Biol. 2008;84(12):1027-33.

ChemSpider CSID:10481938. The free chemical database [Internet]. Royal Scociety of Chemistry [cited 08:02, Jul 30, 2012]. Available from: http://www.chemspider.com/ChemicalStructure.10481938.html

Darzynkiewicz Z, Traganos F, Sharpless T, Melamed MR. Lymphocyte stimulation: A rapid multiparameter analysis. Proc Nati Acad Sci. 1976;73(8):2881-2884.

Darzynkiewicz Z, Bedner E, Smolewski P. Flow cytometry in analysis of cell cycle and apoptosis. Semin Hematol. 2001;38(2):179-93.

Domon M. Cell Cycle-Dependent Radiosensitivity in Two-Cell Mouse Embryos in Culture. Radiat Res. 1980;81:236-245.

Duncan W, Nias AHW. Clinical Radiobiology. 1st ed. Edinburgh: Churchill Livingstone; 1977.

Fenech M, Holland N, Chang WP, Zeiger E, Bonassi S. The HUMN Project – An international collaborative study on the use of the micronucleus technique for measuring DNA damage in humans. Mutat Res. 1999;428:271-283.

Geara FB, Peters LJ, Ang KK, Wike JL, Sivon SS, Guttenberger R, Callender DL, Malaise EP, Brock WA. Intrinsic Radiosensitivity of Normal Human Fibroblasts and Lymphocytes after High- and Low-Dose-Rate Irradiation. Cancer Research. 1992;52:6348-6352.

Ginj M, Hinni K, Tschumi S, Schulz S, Maecke HR. Trifunctional somatostatin-based derivatives designed for targeted radiotherapy using auger electron emitters. J Nucl Med. 2005 Dec;46(12):2097-103.

Goddu SM, Howell RW, Rao DV. Cellular dosimetry: absorbed fractions for monoenergetic electron and alpha particle sources and S-values for radionuclides uniformly distributed in different cell compartments. Journ Nucl Med. 1994;35:303-316.

Grosswendt B. Basic aspects of photon transport through matter with respect to track structure formation. Radiat Environ Biophys. 1999;38(3):147-61.

Gueulette J, Blattmann H, Pedroni E, Coray A, De Coster BM, Mahy P, Wambersie A, Goitein G. Relative biologic effectiveness determination in mouse intestine for scanning proton beam at Paul Scherrer Institute, Switzerland. Influence of motion. Int J Radiat Oncol Biol Phys. 2005;62(3):838-45.

Hall EJ, Giaccia AJ. Radiobiology for the Radiologist. 6th ed. Philadelphia: Lippincott Williams & Wilkins; 2005.

Heimers A. Cytogenetic analysis in human lymphocytes after exposure to simulated cosmic radiation which reflects the inflight radiation environment, Int J Radiat Biol. 1999;75:691.

Henry HF. Fundamentals of Radiation Protection. 1st ed. New York: Wiley-Interscience; 1969.

Howell RW, Narra VR, Sastry KSR, Rao DV. On the Equivalent Dose for Auger Electron Emitters. Radiation Research. 1993;134(1):71-78.

Huber R, Brasselmann H, Bauchinger M. Intra-and-intervidual variation of background and radiation induced micronucleus frequencies in human lymphocytes. Int J Radiat Biol. 1992;61:655-661.

Huber R, Schraube H, Nahrstedt U, Brasselmann H, Bauchinger M. Dose-response relationships of micronuclei in human lymphocytes induced by fission neutrons and by low LET radiations. Mutation Research/Fundamental and Molecular Mechanisms of Mutagenesis. 1994;306(2):135–141.

International Atomic Energy Agency. Cytogenetic Dosimetry: Applications in Preparedness for and Response to Radiation PR-BIODOSIMETRY, IAEA, Vienna; 2011.

International Commission on Radiation Units and Measurements. Fundamental Quantities and Units for Ionizing Radiation, (Report 85). Journal of the ICRU. 2011;11:1.

International Commission on Radiological Protection. The 2007 Recommendations of the International Commission on Radiological Protection, (Publication 103). Ann. ICRP. 2007;37.

Jansen DR, Krijger GC, Kolar ZI, Zonnenberg BA, Zeevaart JR. Targeted radiotherapy of bone malignancies. Curr Drug Discov Technol. 2010;7(4):233-46.

Jones DTL, Symons JE, Fulcher TJ, Brooks FD, Nchodu MR, Allie MS, Buffler A, Oliver MJ. Neutron Fluence and Kerma Spectra of a p(66)/Be(40) Clinical Source. Medical Physics. 1992;19:1285-1291.

Karamychev VN, Reed MW, Neumann RD, Panyutin IG. Distribution of DNA strand breaks produced by iodine-123 and indium-111 in synthetic oligodeoxynucleotides. Acta Oncol. 2000;39(6):687-92.

Kassis AI, Makrigiorgos GM, Adelstein SJ. Implications of radiobiological and Dosimetric studies of DNA-incorporated ^{123}I: The use of the Auger effect as a biological probe at the nanometre level. Radiation Protection Dosimetry. 1990;31(1/4):333-338.

Kassis AI, Wen PY, Van den Abbeele AD, Baranowska-Kortylewicz J, Makrigiorgos GM, Metz KR, Matalka KZ, Cook CU, Sahu SK, Black PM, Adelstein SJ. 5-[125I]iodo-2'-deoxyuridine in the radiotherapy of brain tumors in rats. J Nucl Med. 1998;39(7):1148-54.

Kataoka Y, Sado T. The Radiosensitivity of T and B Lymphocytes in Mice. Immunology. 1975;29:121.

Kellerer AM, Rossi HH. A Generalized Formulation of Dual Radiation Action. Radiation Research. 1978;75(3):471-488.

Knox SJ, Shifrine M, Rosenblatt LS. Assessment of the in Vitro Radiosensitivity of Human Peripheral Blood Lymphocytes. Radiation Research. 1982;89:575-589.

Lacombe F, Belloc F. Flow cytometry study of cell cycle, apoptosis and drug resistance in acute leukemia. Hematol Cell Ther. 1996;38(6):495-504.

Lam GK. On the biophysical interpretation of the mathematical product of dose and relative biological effectiveness. Phys Med Biol. 1990;35(4):481-8.

Laster BH, Shani G, Kahl SB, Warkentien L. The biological effects of Auger electrons compared to alpha-particles and Li ions. Acta Oncol. 1996;35(7):917-23.

Luu QT, DuChateau P. The relative biologic effectiveness versus linear Energy transfer curve as an output-input Relation for linear cellular systems. Mathematical Biosciences and Engineering. 2009;6:3.

Makrigiorgos G, Adelstein SJ, Kassis AI. Auger electron emitters: Insights gained from in vitro experiments. Radiation And Environmental Biophysics.1990;29(2):75-91.

Malaise EP, Lambin P, Joiner MC. Radiosensitivity of human cell lines to small doses. Are there some clinical implications? Radiat Res. 1994;138(1):S25-7.

Mill AJ, Wells J, Hall SC, Butler A. Micronucleus Induction in Human Lymphocytes: Comparative Effects of X-Rays, Alpha Particles, Beta Particles and Neutrons and Implications for Biological Dosimetry. Radiation Research: 1996;145(5):575-585.

Morgenroth A, Dinger C, Zlatopolskiy BD, Al-Momani E, Glatting G, Mottaghy FM, Reske SN. Auger electron emitter against multiple myeloma-targeted endo-radio-therapy with ^{125}I-labeled thymidine analogue 5-iodo-4'-thio-2'-deoxyuridine. Nucl Med Biol. 2011;38(7):1067-77.

Nakahara, T., Yaguchi, H., Yoshida, M. and Miyakoshi, J.. Effects of exposure of CHO-K1 cells to a 10-T static magnetic field. Radiology. 2002;224:817-822.

Niemantsverdriet M, van Goethem MJ, Bron R, Hogewerf W, Brandenburg S, Langendijk JA, van Luijk P, Coppes RP. High and low LET radiation differentially induce normal tissue damage signals. Int J Radiat Oncol Biol Phys. 2012;83(4):1291-7.

Nolte R, Mühlbradt K-H, Meulders JP, Stephan G, Haney M, Schmid E. RBE of quasi-monoenergetic 60 MeV neutron radiation for induction of dicentric chromosomes in human lymphocytes. Radiat Environ Biophys. 2005;44:201-209.

Nolte R, Dangendorf V, Buffler A, Brooks FD, Slabbert JP, Smit FD, Haney M, Schmid E, Stephan J. RBE of 200 MeV neutron radiation for the induction of chromosomal aberrations in human lymphocytes. Proc Sci. 2007;1-10.

Ono K, Masunaga S, Akaboshi M, Akuta K. Estimation of the initial slope of the cell survival curve after irradiation from micronucleus frequency in cytokinesis-blocked cells. Radiat Res. 1994;138(1 Suppl):S101-4.

Pala FS, Alkaya F, Tabakçioğlu K, Tokatli F, Uzal C, Parlar S, Algüneş C. The Effects of Micronuclei with Whole Chromosome on Biological Dose Estimation. Turk J Biol. 2008;32:283-290.

Pizzarello DJ, editor. Radiation Biology. 1st ed. Boca Raton: CRC Press; 1982.

Ryan LA, Wilkins RC, McFarlane NM, Sung MM, McNamee JP, Boreham DR. Relative biological effectiveness of 280 keV neutrons for apoptosis in human lymphocytes. Health Phys. 2006;91(1):68-75.

Savage JRK. Sites of radiation induced chromosome exchanges. Curr Top in Radiat Res. 1970;6:129-194.

Schmid E, Regulla D, Kramer H-M, Harder D. The Effect of 29 kV X Rays on the Dose Response of Chromosome Aberrations in Human Lymphocytes. Radiation Research. 2002;158:771–777.

Schmid E, Schlegel D, Guldbakke S, Kapsch RP, Regulla D. RBE of nearly monoenergetic neutrons at energies of 36 keV and 14.6 MeV for the induction of dicentrics in human lymphocytes. Radiat Environ Biophys. 2003;42(2):87-94.

Slabbert JP, Bins PJ, Jones HL, Hough JH. A quality assessment of the effects of a hydrogenous filter on a p(66)/Be(40) neutron beam. Brit J Radiol. 1989;62:989-994.

Slabbert JP, Theron T, Serafin A, Jones DTL, Böhm L, Schmitt G. Radiosensitivity variations in human tumour cells exposed in vitro to p(66)/Be neutrons and ^{60}Co γ-rays. Strahlentherapie und Onkologie. 1996;172:567-572.

Slabbert JP, Langenhoven JH, Smith, BS. Synthesis of [^{123}I] iodoantipyrine to study the high-LET characteristics of Auger electrons in mammalian cells. Journal of Radioanalytical and Nuclear Chemistry. 1999;240(2):505-508.

Slabbert JP, Theron T, Zölzer F, Streffer C, Böhm L. A comparison of the potential therapeutic gain of p(66)/Be neutrons and d(14)/Be neutrons. Int J Radiat Oncol Biol. Phys. 2000;47(4):1059-1065.

Slabbert JP, August L, Vral A, Symons J. The relative biological effectiveness of a high energy neutron beam for micronuclei induction in T-lymphocytes of different individuals. Radiation Measurements. 2010;45;1455-1457.

Smit BS, Slabbert JP, Reinecke SA, Böhm L. Comparison of cell inactivation by Auger electrons using the two reagents 4-[^{123}I]iodoantipyrine and [^{123}I]NaI. Radiat Environ Biophys. 2001;40(1):47-52.

Sokal, R.R., and F.J. Rohlf. 1995. Biometry. Third Edition. New York: W. H. Freeman.

Sokolov MV, Neumann RD, Panyutin IG. Effects of DNA-targeted ionizing radiation produced by 5-[^{125}I]iodo-2'-deoxyuridine on global gene expression in primary human cells. BMC Genomics 2007;8:192.

Sörén L. Variability of the time at which PHA-stimulated lymphocytes initiate DNA synthesis. Experimental Cell Research. 1973;78:201–208.

Terry SY, Vallis KA. Relationship between chromatin structure and sensitivity to molecularly targeted auger electron radiation therapy. Int J Radiat Oncol Biol Phys. 2012;83(4):1298-305.

Theron T, Slabbert JP, Serafin A, et al. The merits of cell kinetic parameters for the assessment of intrinsic cellular radiosensitivity to photon and high linear energy transfer neutron irradiation. Int J Radiat Oncol Biol Phys 1997;37:423–428.

Thierens H, Vral A, Morthier R, Aousalah B, De Ridder L. Cytogenetic monitoring of hospital workers occupationally exposed to ionising radiation using the micronucleus centromere assay. Mutagen. 2000;15: 245-249.

Thomas P, Tracy B, Ping T, Baweja A, Wickstrom M, Sidhu N, Hiebert L. Relative biological effectiveness (RBE) of alpha radiation in cultured porcine aortic endothelial cells. Int J Radiat Biol. 2007;83(3):171-9.

Todd P. Biological aspects of high LET radiation therapy. Radiology. 1977;125(2):493-6.

Vaidyanathan G, Larsen RH, Zalutsky MR. 5-[^{211}At]Astato-2′-deoxyuridine, an α-Particle-emitting Endoradiotherapeutic Agent Undergoing DNA Incorporation. Cancer Res. 1996;56:1204.

Vandersickel V, Mancini M, Slabbert JP, Marras E, Thierens H, Perletti G, Vral A. The radiosensitizing effect of Ku70/80 knockdown in MCF10A cells irradiated with X-rays and p(66)+Be(40) neutrons. Radiat Oncol. 2010;5:30.

Verhagen F, Vral A. Sensitivity of micronucleus induction in human lymphocytes to low-LET radiation qualities: RBE and correlation of RBE and LET. Radiat Res. 1994;139:208-213.

Vral A, Verhagen F, Thierens H, De Ridder L. Micronuclei induced by fast neutrons versus ^{60}Co γ-rays in human peripheral blood lymphocytes. Int J Radiat Biol. 1994;65:321-328.

Vral A, Fenech M, Thierens H. The micronucleus assay as a biological dosimeter of in vivo ionising radiation exposure. Mutagenesis. 2011;26:11–17.

Wambersie A, Laublin G, Octave-Prignot M, Meulders JP. RBE of d(50)-Be neutrons for induction of chromosome aberrations in *Allium cepa* onion roots. Strahlentherapie. 1979;155(11):776-785.

Warenius HM, Britten RA, Browning PG, Morton IE, Peacock JH. Identification of human in vitro cell lines with greater intrinsic cellular radiosensitivity to 62.5 MeV (p/Be) neutrons than 4 MeV photons. Int J Radiat Oncol Biol Phys. 1994;28:913-920.

Willems P, August L, Slabbert J, Rom H, Oestreicher U, Thierens H, Vral A. Automated micronucleus (MN) scoring for population triage in case of large scale radiation events. Int J Radiat Biol. 2009;1–10.

Wuttke K, Muller WU, Streffer C. The sensitivity of the *in vitro* cytokinesis-block micronucleus assay in lymphocytes for different and combined radiation qualities. Strahlentherapie Onkol. 1998;174:262-268.

Yong K, Brechbiel MW. Towards translation of ^{212}Pb as a clinical therapeutic; getting the lead in. Dalton Trans. 2011;40(23):6068-76.

Zölzer F, Streffer C. Relative Biological Effectiveness of 6 MeV Neutrons with Respect to Cell Inactivation and Disturbances of the G1 Phase. Radiation Research. 2008;169:207–213.